Natural Products

Saxitoxin

*Arun P. Thottumkara, William H. Parsons, and J. Du Bois**

Na⁺

Neuron

K⁺
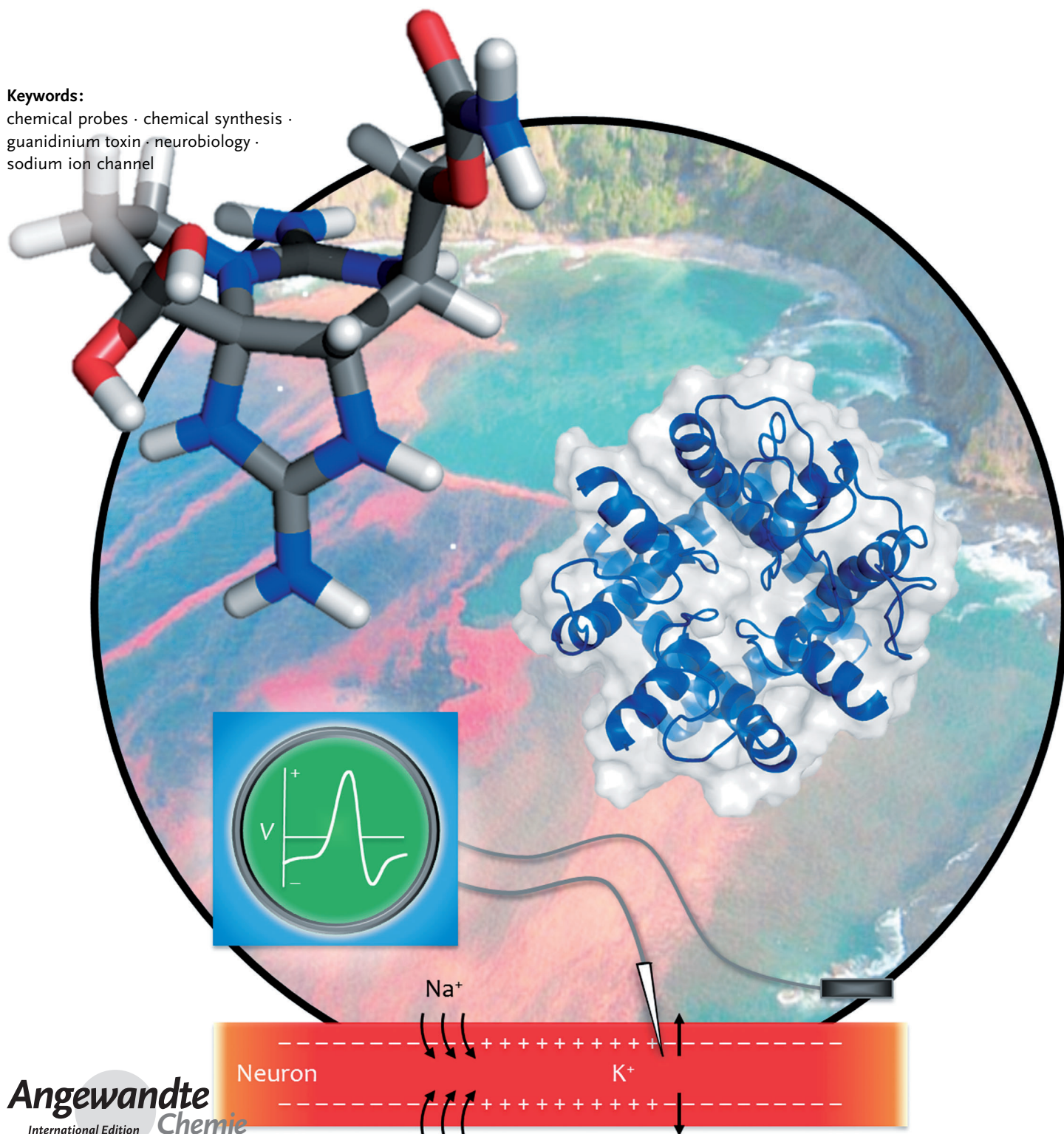
*T*he paralytic agent (+)-saxitoxin (STX), most commonly associated with oceanic red tides and shellfish poisoning, is a potent inhibitor of electrical conduction in cells. Its nefarious effects result from inhibition of voltage-gated sodium channels (Na$_V$s), the obligatory proteins responsible for the initiation and propagation of action potentials. In the annals of ion channel research, the identification and characterization of Na$_V$s trace to the availability of STX and an allied guanidinium derivative, tetrodotoxin. The mystique of STX is expressed in both its function and form, as this uniquely compact dication boasts more heteroatoms than carbon centers. This Review highlights both the chemistry and chemical biology of this fascinating natural product, and offers a perspective as to how molecular design and synthesis may be used to explore Na$_V$ structure and function.

From the Contents

1. Introduction

Neurotoxic agents serve as important chemical tools for understanding protein function associated with the highly complex ionic mechanisms of electrical transmission in cells.[1] The voltage-gated Na$^+$ ion channel (Na$_V$) is a primary site of action for many such poisonous substances. This family of transmembrane proteins is responsible for generating the Na$^+$ current that underlies the initiation and propagation of the action potential in nerve and muscle fibers.[2] Current views on Na$_V$ structure and function are shaped principally from extensive biochemical and electrophysiological investigations along with toxin structure–activity data. The importance of two particular toxin compounds in channel research, namely tetrodotoxin (TTX)[3–6] and saxitoxin (STX),[7] cannot be overstated (Figure 1). Investigations by Narahashi, Moore,[8] Hille, and Armstrong[9] which followed the seminal works of Hodgkin and Huxley[10] to suggest the role of ion channel proteins in modulating electrical current, demonstrated the uniqueness of TTX as a Na$_V$-selective blocking agent. Concurrent studies with STX established this unusual bis-guanidinium compound as a functional equivalent of TTX.[11–13] Both toxins have found extensive use as molecular reagents for characterizing Na$_V$s and as tools in electrophysiology for selective block of sodium currents. Historically, the binding affinity of tetrodotoxin towards individual Na$_V$ isoforms (i.e., nanomolar vs. micromolar) is used to classify channel subtypes as "sensitive" or "resistant." Owing to the uniqueness of TTX and STX in both form and function, the chemical, biological, and pharmacological literature describing these molecules is decidedly vast. This rich history—far from reaching a conclusion—offers an important reminder of the vital role of natural products in discovery research.

The application of small molecules such as TTX and STX as chemical probes for exploring the complex and obligatory role of channel proteins in electrogenesis has been a wellspring of opportunity for both chemical and biological research.[7,14] Given the large body of literature spanned by this topic, we have chosen to focus this Review exclusively on
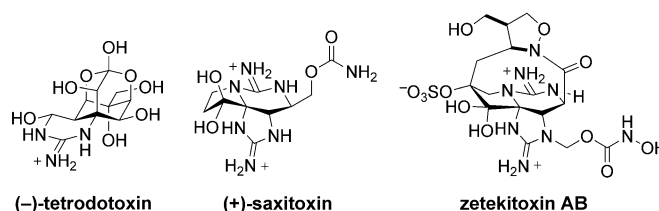

Figure 1. Naturally occurring guanidinium toxins: potent inhibitors of voltage-gated sodium channels.

studies of STX. Saxitoxin is one of now more than 50 related compounds found in Nature and known collectively as paralytic shellfish poisons (PSPs). Its molecular architecture is also represented in zetekitoxin AB, an isolate from the poisonous frog, *Atelopus zeteki*, and an exquisitely potent inhibitor of Na$_V$s.[15] The density of nitrogen atoms expressed in the tricyclic perhydro-pyrrolopurine-based structure of these secondary metabolites offers a number of challenges to the chemist interested in de novo synthesis. The potential for structural derivatization of STX at multiple locales presents a clear advantage over TTX as a starting point for the design of Na$_V$-selective chemical probes. We have attempted to highlight both of these aspects of STX research, which has now spanned more than 50 years. Interested readers of this Review should also consult other recent, comprehensive treatises on this topic.[7,16]

[*] A. P. Thottumkara, Dr. W. H. Parsons, Prof. J. Du Bois
Department of Chemistry, Stanford University
Stanford, CA 94305-5080 (USA)
E-mail: jdubois@stanford.edu

2. Saxitoxin: A Potent Neurotoxin

2.1. A Brief History

Among the most toxic non-protein substances known, the occurrence of saxitoxin can be traced through the medical literature for centuries. The first documented report of paralytic shellfish poisoning was in 1798,[17] and gives an evocative account of a sickness caused by toxic mussels to several crewmembers exploring the Canadian coast of British Columbia. Based on other writings from this period, the poisonous nature of shellfish during certain seasonal periods was recognized among local inhabitants of coastal regions of Alaska, a unique description of which was preserved by Heinrich Johan Holmberg:[18]

> *When we found ourselves in Pogibshii proliv (Peril Strait), we turned to eating mussels (Mytilis) because of a shortage of fresh fish. They must have been poisonous at this time of year for a few hours later more than half of our men died. Even I was near death, but remembering my father's advice, to eat smelt (korushki) at such times, I vomited and recovered my health.*

Saxitoxin and a number of closely related derivatives are produced by a variety of single-celled dinoflagellate algae as well as fresh-water cyanobacteria (Figure 2).[19] The activity of
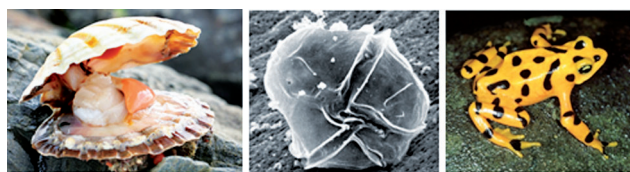

Figure 2. Natural sources of guanidinium toxins: shellfish, the dinoflagellate *Gonyaulax Catenella* (middle), and the Panamanian golden frog *Atelopus Zeteki* (right).

saxitoxin as a paralytic agent was recognized over eighty years ago by Sommer, who first reported lethality data for extracts taken from shellfish along the Pacific Coast of the United States.[20] Filter-feeding mollusks can accumulate the toxins to lethal levels, particularly during algae blooms associated with "red tide" phenomena.[21] Difficulties in collection and measurement of PSPs have led to widely varying figures for the toxic dose of STX for humans. From a series of accidental cases of poisoning, an estimate of 0.5–1 mg of STX is considered the lethal dose for an average-sized person.[22] Shellfish that are known to accumulate PSPs have been found with levels of toxin as high as 20 000 µg per 100 g of flesh (blue mussel, *Mytilus edulis*).[23] The Food and Drug Administration (FDA) considers shellfish having more than 80 µg STX/100 g of flesh unsafe.

The exact cause of paralytic shellfish poisoning was identified in 1927 when Sommer recognized that an outbreak of mussel poisoning off the coast of central California correlated with an observed bloom of *Gonyaulax catenella* (now *Alexandria catenella*), a species of dinoflagellate.[20c,d] Extracts from both mussels and algae showed similar physiological effects including cessation of life when dosed in mice. On the heels of this work, Sommer, with assistance from the US Navy, collected 5000 liters of "red" seawater during an algae bloom near the Monterey Bay. These efforts yielded 90 mg of STX (500 000 mouse units), although separation technology at that time was insufficient for purification of this material.[1a] Subsequent work by Schantz and Sommer to isolate STX from 600 lb of wet siphon taken from Alaskan butter clams proved more efficient as a method for obtaining the poison, and afforded 1.5 g of material. This same procedure enabled scientists at the Biological Laboratories at Fort Detrick, Maryland to obtain 20 g(!) of pure product.[1a]

2.2. Voltage-gated Sodium Ion Channels (Na$_V$)

Access to large quantities of purified STX made possible subsequent efforts to elucidate the molecular basis for its paralytic effects. In the mid-1960s, Evans,[12] Kao and Nishiyama[11] discovered that STX could selectively disrupt sodium currents in excised frog sciatic nerve. Contemporaneous experiments by Narahashi, Moore, and Scott[8] on lobster axon revealed an identical mode-of-action for TTX. The effects of both toxins were shown to occur only when toxin was applied from the extracellular side of the voltage-clamped cell.[8,11,12] These landmark findings were particularly timely, as work by Hodgkin, Huxley and Katz to establish that selective transport of Na$^+$ and K$^+$ underpinned action potential propagation was accomplished with essentially no molecular understanding of ion channel proteins.[9] How Na$^+$ and K$^+$ ions could selectively cross the lipophilic cell membrane was not understood until years later. The specificity of STX and TTX to block Na$^+$ flux (as well as Et$_4$N$^+$ for

Arun Thottumkara was born in 1986 in East Lansing, Michigan and completed his undergraduate studies at Harvard University, where he conducted research in asymmetric catalysis with Prof. Eric N. Jacobsen. He is currently working towards his PhD from Stanford University in the research group of Prof. Justin Du Bois. His work at Stanford centers around the development of new metal-catalyzed carbocyclization reactions and the study of voltage-gated sodium channels in central and peripheral nervous system neurons.

William Parsons was born in 1985 in Fort Knox, Kentucky and completed his undergraduate degree at Williams College, where he conducted research with Prof. Sarah Goh. He obtained his Ph.D. from Stanford University in 2013 working with Prof. Justin Du Bois on the development of saxitoxin-derived molecular probes for the study of voltage-gated sodium channels. At present, he is conducting postdoctoral studies in the lab of Prof. Benjamin Cravatt at The Scripps Research Institute.

selective K^+ channel inhibition) enabled clean separation of the ionic currents, and made possible subsequent research to understand the molecular structure and function of ion channel proteins.

Ion channels are the molecular machines that allow passive diffusion of ions across the cell membrane and are found in all animal, plant and bacterial cells (Figure 3).[2a] Such channels intimately control the movement of Na^+, K^+, Ca^{2+}, and Cl^- ions to produce small, transient changes in ion
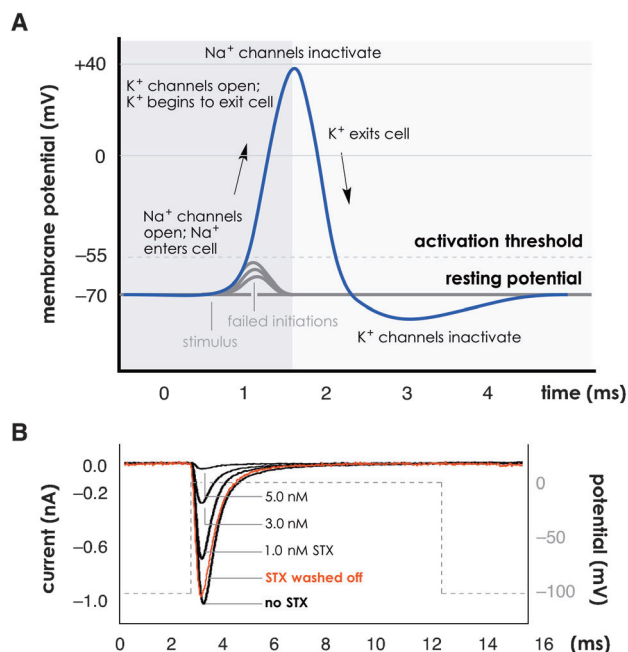

Figure 3. A) An action potential (blue) is the rapid rise and fall in the electrical potential across a cell membrane. The resting membrane potential is initially perturbed by a stimulus that causes a depolarization of the membrane potential above a certain threshold value. In response, Na_V open cooperatively and enable Na^+ ions to enter the cell, causing further depolarization of the cell membrane. This rising phase of the action potential (dark grey region) is accompanied by the opening of voltage-gated potassium channels (K_V). K^+ ions exit the cell in the falling phase (light grey region) of the action potential to re-establish the resting potential. B) Saxitoxin acts as a fully reversible inhibitor of Na_V. A typical current vs. time plot from a whole-cell electrophysiology recording of $Na_V1.4$ expressed in CHO cells. Sodium current is blocked by nanomolar concentrations of STX. Washing the toxin away from the cell restores peak current.

Justin Du Bois received his BS degree from UC Berkeley and was inspired by Ken Raymond and his lab to follow a career in science. He obtained his doctoral degree from Caltech in 1997 under the direction of Erick Carreira and studied as a postdoctoral fellow at MIT with Stephen Lippard. His research interests span methods development, chemical synthesis, and chemical biology. He has been on the faculty at Stanford since 1999.

concentration within cells. These fluctuations are, in turn, coupled to such diverse processes as nerve and muscle excitation, hormonal secretion and sensory transduction.

Voltage-gated sodium ion channels are responsible for the rising phase of the action potential in electrically excitable cells.[2] In response to a stimulus that causes the membrane potential to fluctuate from its resting value, these proteins open cooperatively and allow rapid influx of sodium ions into the cell. Depolarization of the membrane is reversed by voltage-gated potassium ion channels, and ATP-driven Na/K-exchangers maintain the imbalance of Na and K ions against their Nernstian potential. Structurally, Na_V channels exist as a protein complex comprised of a large, pore-forming α subunit and one or more smaller β auxiliary proteins.[24] In mammals, nine distinct isoforms of the pore-forming Na_V α subunit have been functionally expressed, and a tenth sodium channel-like protein (Na_X) has been cloned (Table 1).[2b] The primary amino acid sequences of these

Table 1: Mammalian isoforms of Na_V α-subunits.

Isoform	TTX IC_{50} [nM]	Primary localization	Disease link[a]
TTX-sensitive			
$Na_V1.1$	5.9[28, 29]	CNS,[b] Heart	Epilepsy
$Na_V1.2$	7.8[30, 31]	CNS	Epilepsy
$Na_V1.3$	2.0[31, 32]	Embryonic CNS	Nerve injury
$Na_V1.4$	4.5[31, 33]	Skeletal muscle	Myotonias
$Na_V1.6$	3.8[31, 34]	DRG,[c] CNS	CNS disorders
$Na_V1.7$	5.5[31, 35]	DRG	Pain sensation
TTX-resistant			
$Na_V1.5$	1970[28, 31]	Heart, CNS	Cardiac arrhythmias
$Na_V1.8$	1330[31, 36]	DRG	Pain sensation
$Na_V1.9$	59600[37, 38]	DRG	Pain sensation

[a] This list represents only a partial list of associated disease states. [b] CNS: Central nervous system. [c] DRG: Dorsal root ganglion.

Na_V subtypes are more than 50% identical in the transmembrane and extracellular domains.[2b] The nine Na_V isoforms are characterized by their sensitivity to TTX, with six of the nine functionally expressed isoforms inhibited by nanomolar concentrations of the agent.[2b] Beyond differences in amino acid sequence, variation in channel composition is introduced by RNA editing and splice modifications, protein glycosylation and other post-translational alterations (e.g. phosphorylation, methylation).[25] The association of the pore-forming α-subunit with β proteins offers another means for modulating channel function. Isoforms of both α and β subunits are differentially expressed across various tissue types, as the concentration and profile of Na_V subtypes significantly influences the frequency and amplitude of the action potential output (Table 1).[26, 27]

High fidelity information transfer in electrically excitable cells relies on the proper regulation, discrete subcellular localization, voltage response, and ion gating of Na_Vs. Na_V dysfunction, resulting from factors such as genetic variation, tissue injury or inflammation, can have profound physiological consequences.[39] Disorders of the central nervous system

(epilepsy),[40] heart (long QT and Brugada syndromes),[41] and skeletomuscular system (periodic paralysis, ataxia, dystonia)[42] all have links to problems with Na$_V$ subtype expression and/or channel malfunction.[43] The role of Na$_V$ in pain sensation has received particular attention with the identification of human genetic variants causally linked to severe pain pathologies, which include inherited erythromelalgia (IEM),[44] paroxysmal extreme pain disorder (PEPD),[45] and congenital insensitivity to pain (CIP).[46] The latter renders the individual with whole-body analgesia such that a knife stabbed through the hand or any other part of the body does not elicit a response. Both IEM and PEPD have been ascribed to gain-of-function mutations in single Na$_V$ subtypes expressed principally in sensory neurons (Na$_V$1.7), whereas CIP results from a loss-of-function truncation to the same protein isoform.[46,47] Given these extraordinary human disorders, it is not surprising that Na$_V$ subtypes, which include Na$_V$1.7 in addition to 1.3, 1.6, and 1.8, have become a target of primary interest for next-generation analgesic development.[48]

The design of small molecule modulators of ion channel function that are specific for single Na$_V$ isoforms is a defining challenge of modern-day pharmacological and medicinal chemistry research.[49] Although recent X-ray crystallographic analyses of bacterial sodium ion channels[50–53] should help facilitate small molecule probe and/or drug design, significant structural differences exist between prokaryotic and eukaryotic Na$_V$s. Accordingly, insights gained through toxin binding studies and protein mutagenesis experiments have been instrumental for homology modeling of the α-subunit (i.e., the Na$^+$ conduction pore). Studies with STX, TTX, and related, naturally-occurring congeners are exemplary in this regard. Such efforts have established both toxins as selective "corks" that act to stopper ion flux by lodging in the outer mouth of the channel (so-called Site 1). Electrophysiological measurements of toxin affinities against individual Na$_V$ subtypes have unveiled unique amino acid differences between TTX-sensitive and TTX-resistant channels. A more sophisticated understanding of the interaction between toxin and channel could result in new analogue designs that target specific Na$_V$ subtypes. The availability of STX through de novo synthesis has also yielded modified toxins for use in protein labeling and live cell imaging experiments. Illustrative examples of this work are presented in Section 5.

2.3. The Structures of STX and Its Natural Congeners

Saxitoxin dihydrochloride is a white, hygroscopic material having a molecular formula of $C_{10}H_{19}N_7O_4Cl_2$. Titration studies revealed the diprotic nature of this toxin, giving measured aqueous pK_a values of 8.24 and 11.60.[54] The polar, amorphous nature of STX hampered initial crystallization efforts and attempts at structure elucidation were consigned to chemical degradation studies. Such studies by Rapoport and co-workers culminated in two proposed structures for STX (Figure 4).[55] The task of elaborating the molecular form of STX was daunting given analytical capabilities of the 1960s and the peculiarity of a structure nearly saturated in nitrogen
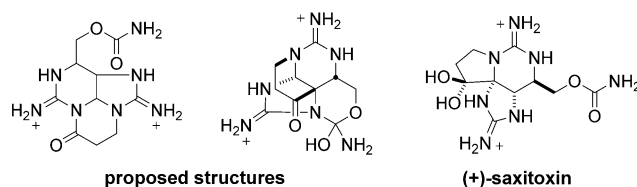

Figure 4. Initial structural proposals[55] for STX and the correct toxin structure, as determined by X-ray crystallography.[56]

atoms, which offers little in the way of signature ^{1}H NMR J-coupling data. It is through this prism that the work of Rapoport's lab should be evaluated. Ultimately, however, X-ray crystal structures of STX derivatives disclosed independently in 1975 by the Clardy/Schantz[56] and Rapoport[55a] labs showed an alternate connectivity, still featuring two guanidinium units and a hydrated ketone. Final confirmation of the structure of STX was provided by Kishi's successful total synthesis in 1977 (see Section 3.1).

Modified forms of STX comprise a large family of natural isolates, the overwhelming majority of which are hydroxylated and sulfated derivatives (Figure 5). As of 2010, 57
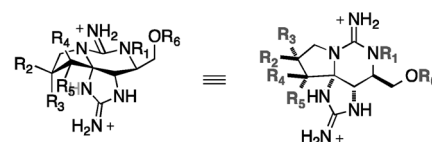
Toxin	R^1	R^2	R^3	R^4	R^5	R^6
STX	H	H	H	OH	OH	C(O)NH$_2$
neo-STX	OH	H	H	OH	OH	C(O)NH$_2$
dcSTX	H	H	H	OH	OH	H
GTX I	OH	H	OSO$_3^-$	OH	OH	C(O)NH$_2$
GTX II	H	H	OSO$_3^-$	OH	OH	C(O)NH$_2$
GTX III	H	OSO$_3^-$	H	OH	OH	C(O)NH$_2$
GTX IV	OH	OSO$_3^-$	H	OH	OH	C(O)NH$_2$
α-STXol*	H	H	H	H	OH	C(O)NH$_2$
β-STXol*	H	H	H	OH	H	C(O)NH$_2$

Figure 5. Select examples of natural and unnatural (*) congeners of STX illustrate structural variation around the toxin core. α- and β-STXol can be prepared through reduction of STX.[59, 60]

discrete structures sharing in common the unique perhydro-pyrrolopurine nucleus have been characterized.[16,57] Collectively, structural modifications occur at one of four locations, C11, C13, N1, and N21. In cases where the affinity of these compounds has been measured against recombinant Na$_V$ isoforms expressed in frog oocytes or mammalian cells (CHO, HEK), introduction of hydroxy or sulfate substituents destabilizes toxin binding. Neosaxitoxin, an N1-hydroxylated congener, is an exception with a measured potency that is approximately equal to that of STX.[58]

Zetekitoxin AB (ZTX), the structure of which was disclosed in 2004, bears a rather extraordinary molecular form.[15e] ZTX is the principal toxic component obtained from skin extracts of poisonous golden frogs collected in Panama in
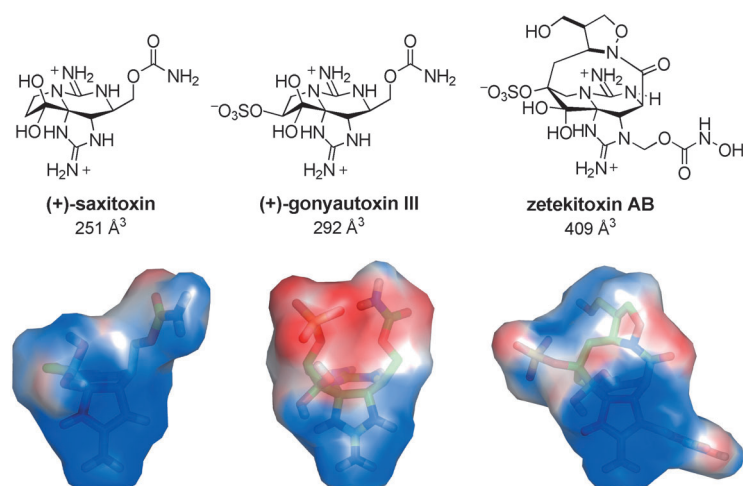
Figure 6. STX, GTX III, and ZTX are proposed to act as outer pore blockers of Na$_V$ despite dramatic differences in both molecular volume (Å^3) and calculated electrostatic potential surfaces. Electrostatic potential surfaces from −1 (red) to +4 (blue) kT.

the 1960s.[15] Owing to the limited supply (300 μg), structural analysis of this material awaited more than 30 years following its isolation and the invention of advanced analytical technologies. Electrophysiology recordings against three Na$_V$ isoforms, 1.2, 1.4, and 1.5, give IC$_{50}$ values of 6.1, 65, and 280 pM, respectively, values that are between 60 and 600 times more potent than STX.[15e] Additional material is needed to further explore the molecular interactions of ZTX with the channel and to determine if this toxin and STX share a common receptor site (Figure 6). The designation of the golden frog, *Atelopus zeteki*, on the IUCN's endangered species list restricts access to a natural source of this material.

2.4. STX Biosynthesis

Early investigations by Shimizu, et al. to deconvolve the stepwise pathway for STX biosynthesis involved feeding radiolabeled amino acids and $^{13}CO_2$ to the dinoflagellate *Alexandrium tamarense* and the blue-green alga *Aphanizomenon flos-aquae*.[61] These insightful studies posited

a Claisen-type condensation of acetate (or a derivative thereof) with arginine. More than 20 years following these experiments, Neilan and co-workers successfully identified a candidate gene cluster for STX biosynthesis in cyanobacterium, *Cylindrospermopsis raciborskii* T3.[62] Analysis of this data suggests a biosynthetic route for the production of STX that is consistent with Shimizu's feeding studies, and implicates arginine and acetyl-CoA as well as S-adenosylmethionine and carbamoyl phosphate as STX biosynthetic precursors (Scheme 1).

Following this initial report, gene clusters encoding for STX have been identified in disparate strains of cyanobacteria as well as dinoflagellates.[63] Saxitoxin is rather unusual in this regard, as a toxin that is synthesized by organisms from two different kingdoms of life—a finding that has captured the attention of evolutionary biologists.[64] These recent reports have also reignited interest in the biosynthetic production of TTX (although a candidate gene cluster for this toxin has not yet been identified).[4]

As of the writing of this Review, the protein products of the genes responsible for producing STX have not been isolated and characterized. As such, a method for in vitro preparation of this toxin and engineered analogues is currently beyond reach.[65]

3. De Novo Synthesis of Saxitoxin

The storied history of STX as a target for natural product synthesis is as rich in detail as the molecule itself. Recent efforts to synthesize the toxin have been motivated, in part, by opportunities to exploit the de novo production of this toxin for the purpose of generating selective tools for investigations of Na$_V$. A comparative review of the unique approaches for assembling STX, as presented below, should impress upon the reader the versatility of the perhydro-pyrrolopurine core as a molecular template for analogue development. In the context of molecular design, this point is worth emphasizing as it draws an important distinction from TTX—arguably the more prominent of the two toxins in Na$_V$ research. The structure of TTX comprises a polysubstituted, polyoxygenat-
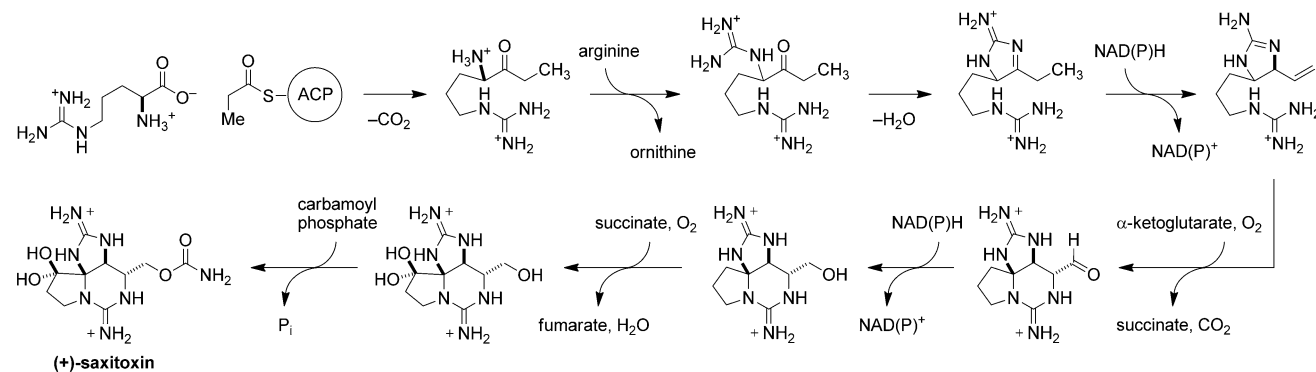
Scheme 1. Proposed biosynthetic pathway for STX in cyanobacterium *C. raciborskii* T3.[62b]

ed cyclohexane frame that leaves no carbon unmodified. Based on Na$_V$ inhibition studies with naturally occurring, deoxygenated congeners of TTX, the large degree of oxygenation appears critical for potency.[66] By contrast, decarbamoylated STX (dcSTX) and other C11 and C13 variants retain the ability to block Na$_V$ at low nanomolar concentrations. Analysis of the known chemical syntheses of STX and TTX offers a second point of contrast. Available technologies for preparing TTX are effectively twice that in length to STX (ca. 30 vs. 15 steps), a considerable impediment to analogue production. These factors advantage STX as a "blueprint" for Na$_V$ tool design.

As a problem in de novo chemical synthesis, the unassuming molecular size of STX belies its intricate challenges. The charged, polar bis-guanidinium functional groups and weak chromophoric property of the toxin complicate isolation and purification of small quantities of material. The tricyclic frame, bearing an unusual aminal moiety (C4), boasts a small phalanx of heteroatoms that number more than carbon, a rarity among known secondary metabolites. When disassembled to its component parts, the C4 aminal reveals a ketone group, which is flanked on one side by a second ketone (C12) and on the other by three contiguous substituted carbon centers (C5, C6, C13). The four completed syntheses of STX and two of the closely related C11-sulfated form, GTX II/III, each present a novel solution to the problems posed by the complex molecular architecture of the toxin. In the aggregate, these works highlight a list of significant advances in the practice of organic chemistry, culminating in preparative methods for STX assembly and enabling new opportunities in Na$_V$ research.

3.1. Kishi (1977)

The landmark synthesis of racemic STX in 1977 by Kishi and co-workers was completed a mere two years following the disclosure of the X-ray crystal structure.[67] The difficulties intrinsic to handling and purifying compounds of such polarity and the limited analytical capabilities of the time make this work all the more impressive. At a strategic level, the Kishi synthesis is able to avoid some of the complications associated with the guanidinium groups by installing these units at an advanced stage in the synthetic route. As Kishi notes, "the reason for postponing the introduction of the guanidino groups to the very late stage of the synthesis was to avoid as much as possible technical difficulties in handling the very basic, polar guani-

dine derivatives."[67b] Two electrocyclic processes are featured in the assembly of a tricyclic thiourea **1**, which serves as a key intermediate in the overall scheme (Figure 7).

The preparation of urea **1** commences from γ-aminobutyric acid, which is processed in eight steps to thiolactam **4** (Figure 8). A shorter sequence featuring an ester enolate-
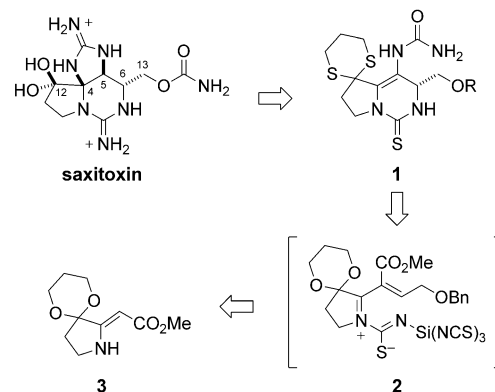

Figure 7. Retrosynthetic analysis of Kishi's route to (±)-STX.

nitrile addition reaction (Blaise reaction) provides the analogous dithiane derivative.[67b, 68] Following the precedent of Eschenmosher,[69] coupling between **4** and α-bromo-β-ketoester **5** affords vinylogous carbamate **3**. Unlike traditional sulfide contraction processes, conversion to **3** occurs in the absence of a thiophilic reagent. Subsequent transformation of this material to thiourea **6** is a particularly notable step, which exploits Si(NCS)$_4$, a reagent that has found sparing use in organic synthesis since its introduction by Neville in 1963.[70] Ring closure is suggested to occur through 6π-electrocyclization of intermediate **2**, and establishes the first of three requisite stereocenters. Following completion of the racemic STX synthesis, a modification of this sequence using (R)-glyceraldehyde acetonide in place of benzyloxyacetaldehyde was shown to afford the thiourea product **10** in a 9:1
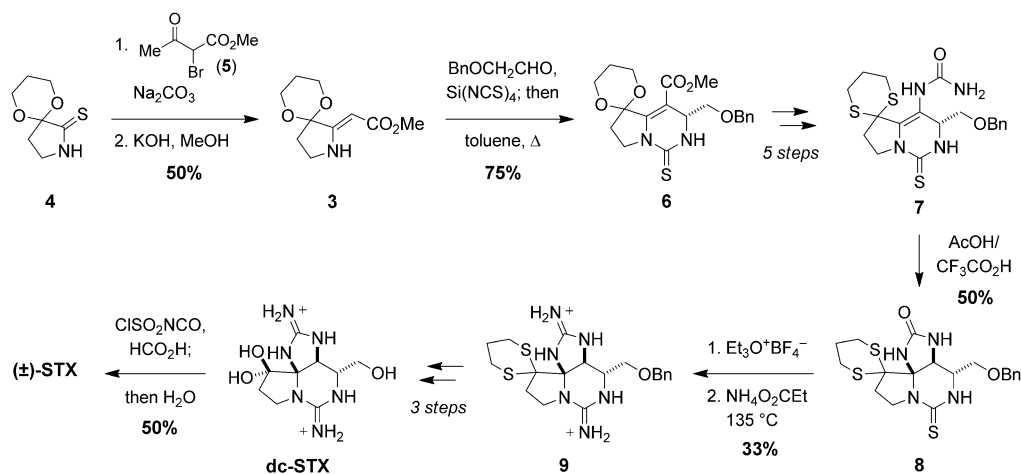

Figure 8. The first disclosed synthesis of (±)-STX.

diastereomeric ratio (Figure 9). This tactical advance enabled completion of an asymmetric synthesis of (−)-decarbamoyl-saxitoxin, the unnatural antipode of the natural product.[71]
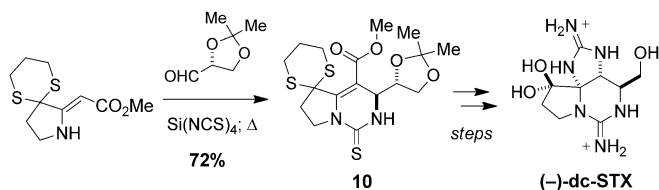

Figure 9. Electrocyclization with (*R*)-glyceraldehyde enables asymmetric synthesis of (−)-dcSTX.

The finished synthesis of (±)-STX follows from thiourea **7** through a sequence of functional group manipulations, highlighted by acid-promoted ring closure to forge the third ring of the tricyclic skeleton (Figure 8). It is postulated that this step may also occur through a concerted pericyclic process. Remarkably, the desired product **8** is generated in 50% yield with only 10% of the accompanying diastereoisomer. A subtle conformational bias induced by the lone C6-stereocenter may explain the apparent torquoselectivity of this electrocyclization reaction.

Successful preparation of the key bis-urea intermediate **8** gives way to (±)-dcSTX en route to the target molecule. The transformation of the two urea groups to the bis-guanidinium product **9** occurs under forcing conditions (135°C)[67] and is modestly efficient. Installation of the necessary C13 carbamate group on dcSTX is performed in neat formic acid and is also somewhat capricious. This end-game sequence is thus limiting with respect to analogue preparation, particularly with regard to modification of the substituent group at C13. Nevertheless, the laudable achievement by the Kishi lab as the first to prepare STX and later (−)-dcSTX has produced a timeless piece of work.

3.2. Jacobi (1984)

Jacobi and co-workers have delineated a racemic synthesis of STX that is impressive in both design and brevity.[72] Inspired by Kishi's report, bis-urea **11** was targeted as a critical intermediate (Figure 10). Completion of the synthesis from this compound would leverage the last five steps of the Kishi plan, proceeding through (±)-dcSTX in the penultimate step.[67a] Recognition that **11** could be accessed through reductive N-N cleavage of hydrazide **12** is truly inspired, and reduces the problem of synthesizing the tricyclic frame of STX to a dia-
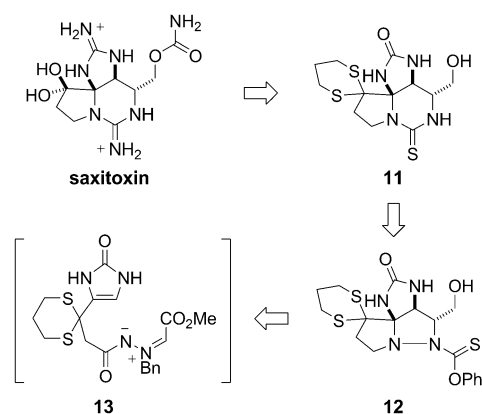

Figure 10. Jacobi's path to (±)-STX featuring a [3+2]-azomethine ylide cycloaddition reaction.

stereoselective intramolecular [3+2] cycloaddition of azomethine ylide **13**.

Preparation of the cycloaddition precursor **15** is achieved starting from imidazolin-2-one **14** (Figure 11); this commercial starting material is readily elaborated to the desired hydrazide. Condensation of this nucleophile with methylglyoxylate hemi-acetal generates a reactive azomethine imine **13**, which cycloadds across the tethered imidazolinone to furnish the [3+2] adduct. The reaction proceeds with extraordinary selectivity to give **16** as a single product.[73] A rationalization for this stereochemical outcome posits a destabilizing interaction between the methyl ester and benzyl groups in the transition structure (**16-α**$^+$) leading to the alternate isomer (**16-α**, Figure 12). The fact that the tricyclic product preferentially forms with the incorrect stereochemistry at C6 does not detract from the simple elegance of this transformation. The ester is easily epimerized with NaOMe to favor the α-configured product with ≥ 98:2 selectivity at thermodynamic equilibrium, and can be reduced to alcohol **17** without isolation.

The synthesis of bis-urea **11** is enabled from **17** through four high yielding steps that include selective BH₃-mediated hydrazide reduction to furnish **18**, followed by N-debenzylation and hydrazine acylation to afford *O*-thiocarbamate **12**. Finally, reductive N-N cleavage is effected with Na in NH₃;
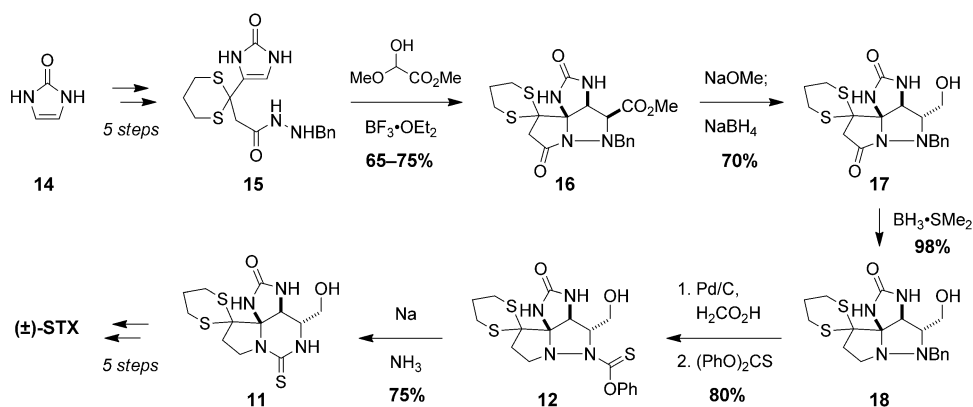

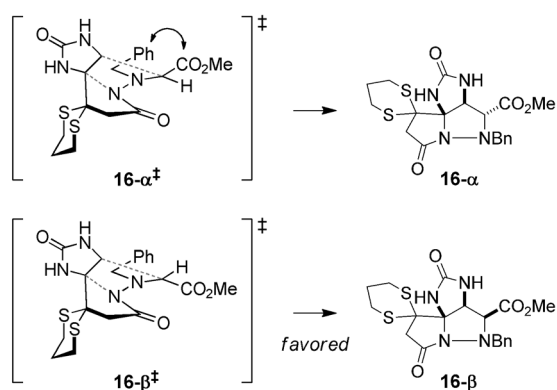***Figure 11.*** The Jacobi synthesis of (±)-STX.

Figure 12. Stereochemical rationalization for exclusive formation of **16-β**.

concomitant ring closure of the six-membered thiourea gives **11**. Protection of the C13 alcohol as the acetate ester is followed by simultaneous conversion of the urea groups to the bis-guanindium species under conditions described by Kishi. Decarbamoylsaxitoxin is thus produced in 0.5–1 g quantities without recourse to chromatographic purifications throughout the entire sequence! It is difficult to envision a more facile entry to racemic saxitoxin than the stereocontrolled azomethine imine strategy outlined by Jacobi, and perhaps surprising that no report has appeared describing the use of an asymmetric catalyst or chiral auxiliary to control the absolute sense of induction in this [3+2] reaction. In its entirety, the Jacobi route to STX offers a masterclass in natural products synthesis.

3.3. Nagasawa (2009)

Like the work of Jacobi, studies by Nagasawa and co-workers aimed at the preparation of STX highlight the clever application of dipolar cycloaddition-based strategies for the preparation of nitrogen heterocycles.[74] In this case, however, combining an optically active nitrone **21** with nitroalkene **22** affords an enantio-enriched isoxazoline product **20**, thereby enabling access to a single antipode of the natural product (Figure 13). Another key component of the Nagasawa

strategy is the exploitation of an intramolecular condensation reaction to close the 5-membered ring guanidine, which biases the correct stereochemical outcome at C4. This reaction is planned in the late-stage of the synthesis, and parallels a related approach by Du Bois (see Section 3.6).[75]
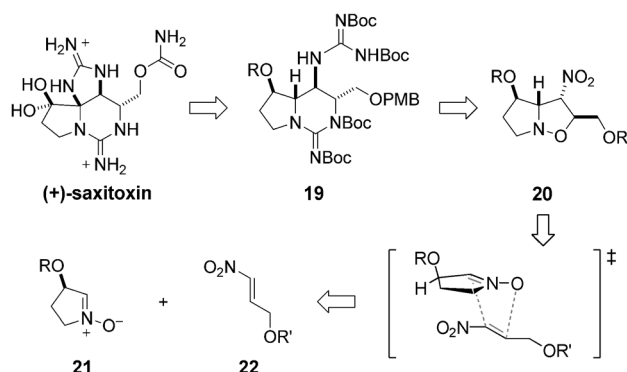

Figure 13. The Nagasawa strategy towards (+)-STX.

Nitrone **23** is available in five steps from L-malic acid and easily accessible in multigram quantities.[76,77] Stirring this dipole with nitroalkene **24** in the absence of solvent generates the appropriate isoxazoline with complete diastereocontrol. The stereochemical outcome of this reaction is consistent with a favored-*endo* transitition state (Figure 13) in which the approach of the nitroalkene is opposite the sterically large siloxy group. Treatment with DBU epimerizes the C5 position to the necessary configuration (Figure 14). Notably, reduction of this material with Zn is selective for converting the nitro moiety to the corresponding hydroxylamine without cleaving the N–O bond of the heterocycle. Process optimization has led to an improved one-pot, three-step sequence to prepare hydroxylamine **25** from nitrone **23** (Figure 14).

From isoxazoline **25**, it is possible to access a bicyclic structure (**26**) that encodes one of the two requisite guanidine moieties of the natural product (Figure 14). Selective α-hydroxylation of the C12 ketone using o-iodoxybenzoic acid (IBX) in DMSO is a signature maneuver in the Nagasawa route to STX and delivers the hemi-aminal product in 94 %.
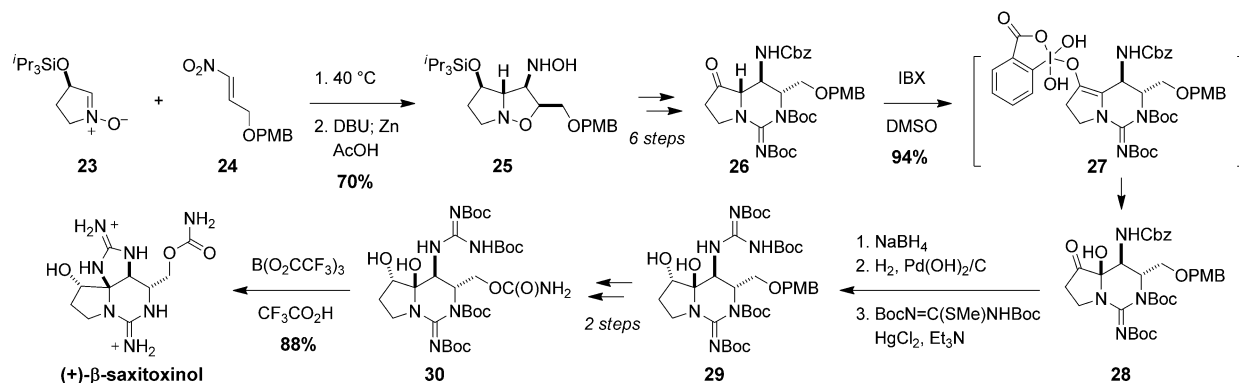

Figure 14. A path to (+)-STX featuring selective α-ketone oxidation.

The remarkable selectivity noted in this reaction is believed to result from intramolecular oxidation of an enolic hypervalent iodine species such as **27**. Hemi-aminal **28** is configured appropriately for ring closure of the 5-membered guanidine. In practice, however, attempts to form the aminal at C4 were foiled by the presence of the C12 ketone. Accordingly, reduction of the C12 ketone in **28** was necessitated.

Hemi-aminal **28** is surprisingly stable under reductive conditions and can be subjected to hydrogenolysis to cleave the Cbz-protecting group. Selective guanidinylation of the C5 amine yields **29**; PMB group removal and carbamoylation affords **30**, which can be converted to the tricyclic core of STX through a Lewis acid-promoted condensation reaction. The final sequence of steps to generate (+)-β-saxitoxinol, a re-

duced form of the natural product, follows the Du Bois synthesis[75] and relies on a method described by Koehn, et al.[59] for oxidation of the C12 carbinol to generate (+)-STX.

Highlights of the Nagasawa synthesis of (+)-STX include the diastereoselective nitrone cycloaddition and IBX-mediated selective oxidation of C4. It is also notable that a strategic decision to forego the use of urea or thiourea dertivatives as guanidine surrogates avoids added steps and modest yields inherent to such functional group exchange reactions. Similar logic underscores the STX preparations described by Du Bois,[75] Looper,[78] and Nishikawa.[79] The versatility of the Nagasawa route has enabled the preparation of non-natural forms of STX (as discussed in Section 5.2) as well as (+)-gonyautoxin III, a C11-sulfated derivative initially isolated from dinoflagellate, *Gonyaulax tamarensis* (Figure 15).[77]

3.4. Looper (2011)

Studies by Looper and co-workers to develop general methods for cyclic guanidine formation from propargylic derivatives have demonstrated the power of reagent control for influencing regioselectivity and ring size in these types of reactions.[80] This technology is optimally suited for crafting (+)-STX, effectively unraveling the complex tricyclic core to a much-simplified acyclic structure **33** (Figure 16). This alkyne-substituted derivative can be easily obtained from serine-derived aldonitrone **34**, following earlier precedent.[75b,81] In keeping with investigations by Du Bois and Nagasawa, the Looper synthesis is predicated on the direct installation of both guanidine units. The ability to employ an alkyne functional group as a C4,C12 α-diketone surrogate and to utilize C5 and C6 as stereochemical controlling elements for selective aminal formation results in a beautifully streamlined assembly of the toxin. The Looper synthesis is further distinguished from others in that the pyrrolidine ring is the last of three rings formed.

Diastereoselective magnesium acetylide addition to nitrone **34** occurs smoothly to furnish a 9:1 mixture of *anti/syn*-configured products (Figure 17). Four steps are needed to
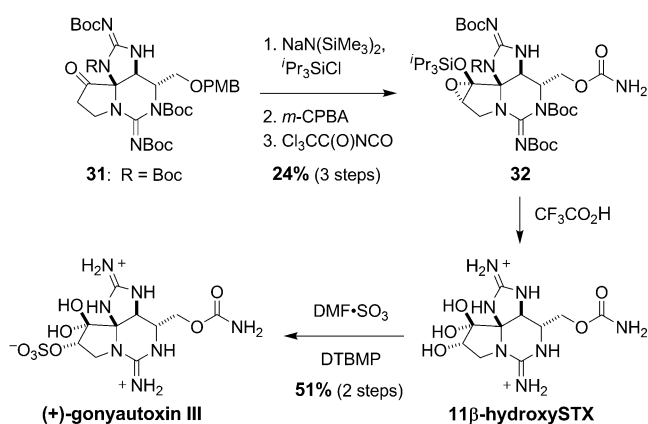

Figure 15. An alternative end-game strategy affords (+)-GTX III. DTBMP = 2,6-di-*tert*-butyl-4-methylpyridine.
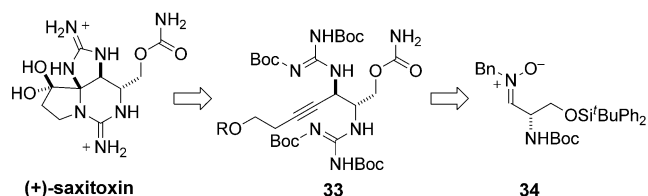

Figure 16. Alkyne oxidative cyclization highlights the Looper synthesis of (+)-STX.
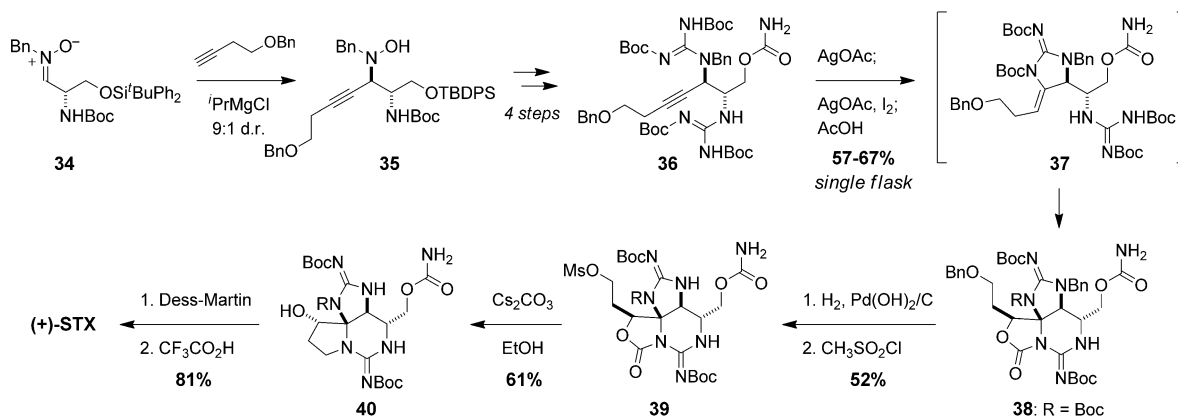

Figure 17. A sequential three-step, one-pot tricyclization reaction transforms an acyclic starting material into the core structure of STX.

transform this material **35** into the Boc-protected bis-guanidine **36**, which includes the requisite C13-carbamate group found in the natural product. Regioselective formation of 5-*exo*- or 6-*endo*-dig guanidine isomers is controlled by judicious choice of metal catalyst for inducing the cyclization event. In this particular case, the 5-membered ring product **37** was formed in near quantitative amounts with 10 mol% AgOAc. While attempts to trigger the second ring closure using epoxidizing agents did not prove fruitful, the combination of I_2 and AgOAc

Figure 19. A path to (+)-dc-α-STXol through sequential alkyne oxidation reactions.

was sufficiently reactive to produce the desired outcome. Finally, exposure of **37** to a third successive treatment of AgOAc effected intramolecular displacement of the secondary iodide and oxazolidinone **38** formation. The dependence of AgOAc in these three steps has been utilized to great benefit in an optimized protocol that directly transforms **36** to **38** in a single reaction flask. The elegant cascade of events promoted by AgOAc transforms the unassuming acyclic material through a pathway in which two C-N, one C-O, and three new rings are forged.

The Looper synthesis of (+)-STX is completed from **38** in five efficient transformations, punctuated by a single step oxazolidinone hydrolysis/pyrrolidine ring forming reaction. This feat is accomplished from mesylate **39** using ethanolic Cs_2CO_3;[82] alcohol oxidation and guanidine deprotection provide the natural product. All told, the finished route to (+)-STX offers a modern view of chemical synthesis that exploits transition-metal catalyzed reactions to control chemo- and regioselectivity. The brevity of the synthesis, the protecting group strategy and the ability to access a guanidine-protected form of STX should prove amenable for preparing other PSP derivatives.

3.5. Nishikawa (2011)

Nishikawa and co-workers have advanced a synthesis of naturally occurring (+)-decarbamoyl α-saxitoxinol, a derivative of saxitoxin produced by cyanobacteria.[79] This work finds similarities to that of Looper, in that an alkyne group is used as a proxy for the C4,C12-diketone (Figure 18).[78] Formation of guanidine **41** is possible through alkyne oxidation and intramolecular cyclization.

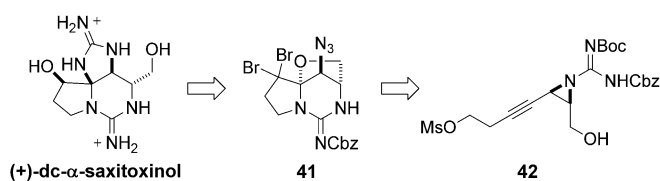Commencing from a serine-derived aldehyde **43** (Garner's aldehyde), azide **44** is prepared through a straightfor-

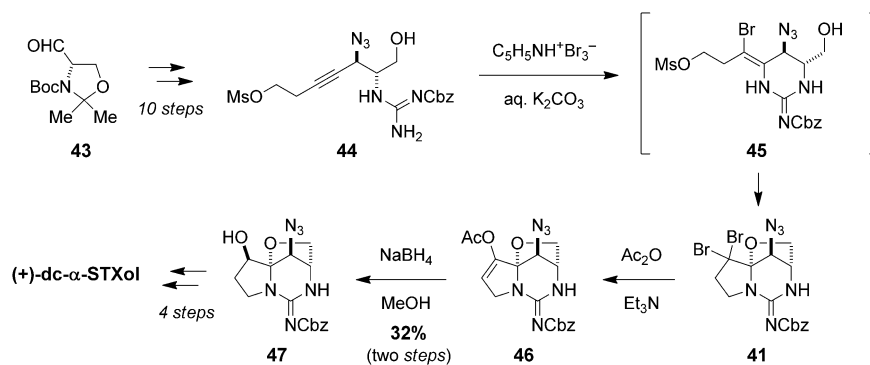**Figure 18.** Nishikawa's analysis of (+)-decarbamoyl-α-STXol.

ward ten step protocol (Figure 19).[83] Treatment of this compound with pyridinium tribromide ($PyHBr_3$) under biphasic conditions initiates a cascade sequence that renders aminal **41** as the final product. In this transformation, alkyne bromination triggers guanidine cyclization to generate the first of three rings. A second bromination of the intermediate alkene **45** is utilized to effect N,O-acetal formation; pyrrolidine closure then follows through intramolecular C10-mesylate displacement. The reactivity of $PyHBr_3$ appears to be uniquely suited to this process, as other conventional brominating agents (e.g., N-bromosuccinimide) fail to give the desired outcome.[83] *gem*-Dibromide **41** is converted to enol acetate **46** in an unusual process employing acetic anhydride and triethylamine.[79] Reduction of this intermediate with $NaBH_4$ affords the α-C12 alcohol **47** as a single diastereomer. The desired toxin can be reached from **47** in just four steps through a sequence that exploits $B(O_2CCF_3)_3$ to promote five-membered guanidine ring formation (see Sections 3.3, 3.6). Accordingly, a complex problem in cyclic stereocontrolled synthesis is efficiently solved through the creative application of an oxidative cascade, which commences from a readily prepared acyclic material **44**.

3.6. Du Bois (2006, 2007, 2008)

The first asymmetric route to STX was delineated by Fleming and Du Bois[75a] nearly three decades after Kishi reported the cardinal synthesis. The synthetic planning was done with knowledge of the importance of STX as a tool in ion channel research and with the expectation that de novo preparation of the toxin could be leveraged for studies of Na_V molecular structure and cellular function. Methods advances in C-H amination, alkene oxidation, and guanidine functionalization have culminated in the development of two entirely disparate routes to the bis-guanidinium tricyclic core of the PSPs. Together, these processes can deliver substituted toxin derivatives at N1, N7, N9, N21, C10, C11, and C13.[60,84–88]

As noted previously, the adjacent C4 and C12 carbons in STX mask a vicinal diketone. In considering surrogate functional groups for this moiety, an alkene or alkyne are evident candidates. The former can be easily embedded in a medium-sized ring **48** that encodes both C5 and C6 stereocenters (Figure 20). Such a plan is intended to capitalize
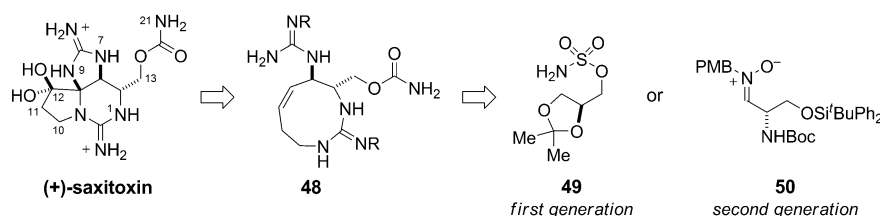
5770 www.angewandte.org

© 2014 Wiley-VCH Verlag GmbH & Co. KGaA, Weinheim

Angew. Chem. Int. Ed. **2014**, *53*, 5760–5784

Figure 20. Retrosynthetic disconnection of (+)-STX to a monocyclic bis-guanidine.

specialized, as other oxidant combinations such as OsO_4 and $tBuOOH$ furnish the isomeric bicycle **59**. While the factors that control selectivity in this unusual four-electron alkene oxidation remain opaque, the correct product is readily transformed to β-saxitoxinol upon treatment with B-$(O_2CCF_3)_2$. This Lewis acid promotes

on the conformational bias of **48** to control the stereochemical outcome of C4-aminal formation. The challenges presented in this disconnection strategy require methods for 1) six-electron alkene oxidation to generate the requisite C4,C12-diketone, and 2) preparation of the unusual 9-membered ring guanidine.

Two routes have been outlined by the Du Bois lab for preparing cyclic guanidine **48** (Figure 21).[75] One uses Rh-catalyzed C-H amination technology[89] for the stereoselective synthesis of oxathiazinane **51**, a novel heterocyclic unit that masks a 1,3-amino alcohol.[90] Elaboration of this compound to isothiourea **53** is followed by sequential azide reduction/carbodiimide formation/ring closure to furnish **54**. The nine-membered guanidine is an unprecedented structure, available in 65% through this one-flask, tandem series of events.

The effectiveness of oxathiazinane **51** en route to **54** notwithstanding, a shorter, readily scalable process for generating this compound is available from the L-serine-derived nitrone **50** (Figure 21).[75b] Acetylide addition of **55** to **50** introduces the necessary isothiourea, thus reducing the total number of steps for accessing **57**. This material is easily processed through a cyclocondensation reaction to **54**.

Despite the limited number of reaction methods for direct alkene oxidation to prepare α-ketol or α-diketone structures, a combination of catalytic $OsCl_3$ and Oxone proved successful for regioselective keto-alcohol formation from carbamate **58** (Figure 22). The C4-ketone, however, is not obtained, as transannular addition of the guanidine N3-nitrogen is strongly favored and gives bicyclic hemi-aminal **60** as a single epimer. The conditions used for formation of this product are rather
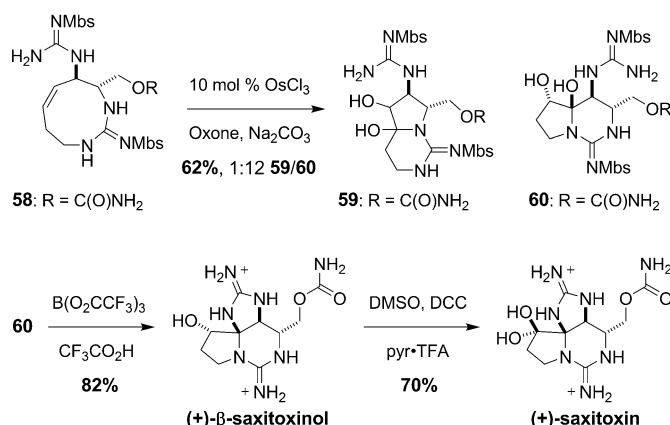
Figure 22. The end-game sequence for alkene oxidation and ring-closure.

both ring closure of the 5-membered guanidine and cleavage of the methoxybenzenesulfonyl (Mbs) protecting groups. Oxidation of β-saxitoxinol is achieved using a dicyclohexyl-carbodiimide/DMSO protocol described previously.[59] The completed synthesis of (+)-STX has enabled access to unnatural derivatives of the toxin, primarily those substituted at N21 of the carbamate group (see Section 5.3).

A desire to prepare STX congeners, GTX II, GTX III, and ZTX, as well as STX-structures modified at C10 and C11 prompted efforts by the Du Bois lab to develop an alternative synthesis of the perhydro-pyrrolopurine core structure common to these targets (Figure 23). Available reaction technology for generating electrophilic nitrenoid oxidants

Figure 21. First and second generation syntheses of an unusual nine-membered ring guanidine intermediate.

Figure 23. An alternative pathway to PSPs capitalizing on metal-catalyzed pyrrole oxidation.

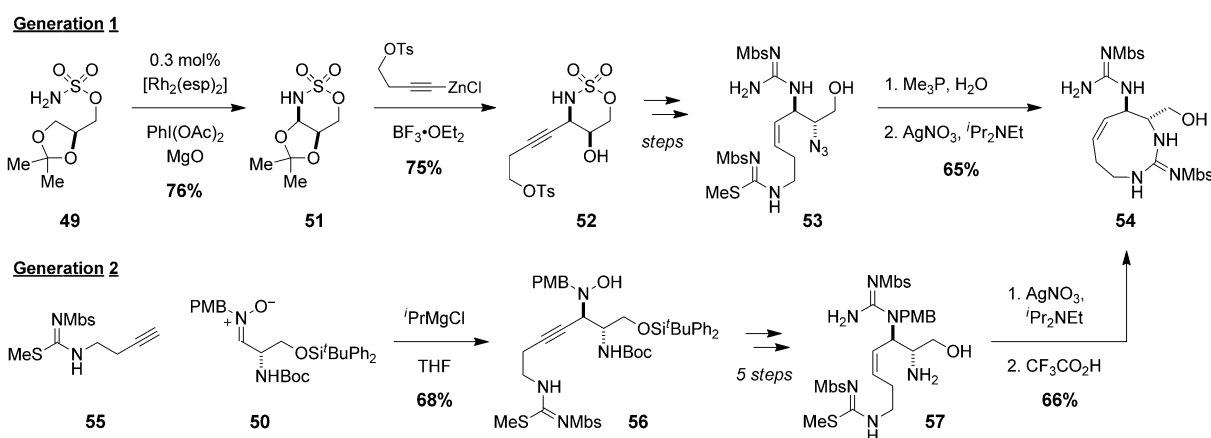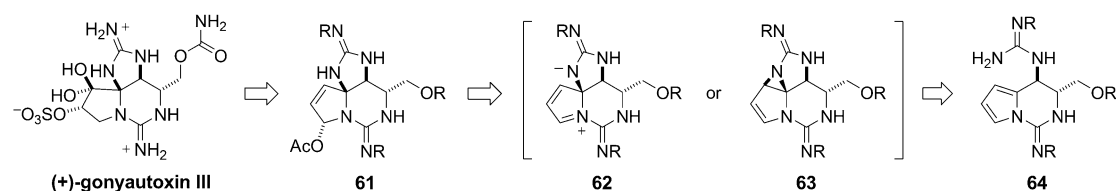inspired a plan that would capitalize on pyrrole oxidation to generate the tricyclic N,O-acetal **61**. This intermediate is appropriately configured for installing both the requisite C11-substituent and C12-ketone groups for either GTX or ZTX assembly.

Asymmetric synthesis of (+)-GTX III follows from L-serine methyl ester **65** (Figure 24), which is transformed in four steps to urea **67** through a sequence that exploits a diastereoselective Pictet-Spengler-type addition reaction (>20:1 trans/cis). The resulting amine **67** is processed to the bis-guanidine **68** using conventional tactics for installing both
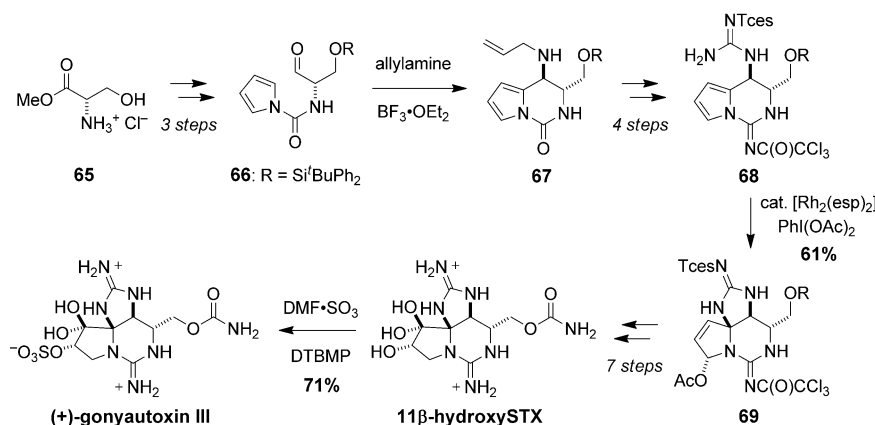
3.7. Synopsis

The unique polycyclic, heteroatom-rich structure of STX and related PSPs remains a fascinating, contemporary challenge for chemical synthesis. The multiple routes that have been advanced for the preparation of these toxins are distinguished from one another and mark an evolution in the development of reaction technologies for constructing nitrogen heterocycles and guanidine derivatives. These efforts have culminated in asymmetric syntheses of (+)-STX and (+)-GTX III that are amenable to the production of select derivatives for studies of both Na_V structure and function, as discussed in the ensuing sections. The desire for molecular probes patterned after STX should encourage future innovations in synthesis to further streamline the preparation of these complex reagents. And as the structures of new STX congeners such as ZTX are revealed, interest in the guanidinium toxins is certain to remain high.

Figure 24. The first completed synthesis of (+)-GTX.

4. Defining the Toxin Binding Site in Na_V

Investigations with STX and TTX have been of central importance in defining both cellular and molecular features of Na_Vs. The large size (ca. 260 kDa) of the pore-forming α-subunit of the mammalian sodium channel, the extent of glycosylation (15–30% by weight),[25c] and its obligatory placement in the cytoplasmic membrane of cells complicate the isolation of sufficient quantities of the protein for structural studies. Crystallographic analyses of bacterial and mammalian voltage-gated K⁺-channels[92] and prokaryotic Na_Vs[50] have facilitated the construction of homology models of mammalian Na_V orthologues; the faithfulness of such models, however, is tested by low sequence homology and the homotetrameric form of these other channels. The availability of a 19 Å cryoelectron image of Na_V taken from *Electrophorus electricus*, while offering a rather provocative view of the gross topology of the protein and ion conductance portals,[93] lacks sufficient resolution to offer molecular insights into Na_V form and function. Accordingly, current views of Na_V structure are shaped through experiments that include recombinant expression of Na_V, protein site-directed mutagenesis, electrophysiology, and toxin SAR data.

functional groups. Protection of the N-7.8.9-guanidine as the N-trichloroethoxysulfonamide (Tces) is required for subsequent nitrenoid generation. Pyrrole oxidation takes place under the action of a dirhodium tetracarboxylate catalyst and hypervalent oxidant to give the pyrroline product **69**. In the event, **69** is obtained as a single diastereomer, having formed as the result of either trapping of a dipolar species **62** or ring opening of aziridine **63** with AcOH (Figure 23). N,O-Acetal **69** is a versatile intermediate for elaborating the C10, C11, and C12 positions of the pyrrolidine ring and, because of the differential protection of the two guanidine groups, for modifying N1, N7 and N9. Completion of the first synthesis of GTX III proceeds through 11β-hydroxySTX; selective C11-OH sulfation of this compound using DMF·SO₃ and a pyridine base affords the natural product. Upon standing in aqueous soution at slightly alkali pH, epimerization of the C11-sulfate occurs to give a 3:1 mixture of GTX II/III. Such a finding is in agreement with the original isolation work of these molecules.[91]

5772 www.angewandte.org

© 2014 Wiley-VCH Verlag GmbH & Co. KGaA, Weinheim

Angew. Chem. Int. Ed. **2014**, *53*, 5760–5784

4.1. The Structure of the Eukaryotic Na$_V$ Channel

In 1984, Noda and colleagues reported the complete amino acid sequence of the sodium channel from the electroplax of *Electrophorus electricus*.[94] These seminal findings identified the functional α-subunit of the channel as a large 260 kDa single polypeptide with four homologous repeats. In subsequent investigations, Guy and Seetharamulu posited a sophisticated model of the secondary and tertiary structure of the protein based on analysis of the sequence.[95] Each domain is comprised of six α-helices (S1–S6) spanning the length of the membrane, including an arginine-rich helix (S4) that functions as a voltage-sensor[96] in response to changes in membrane potential (Figure 25). Large intracellular loop
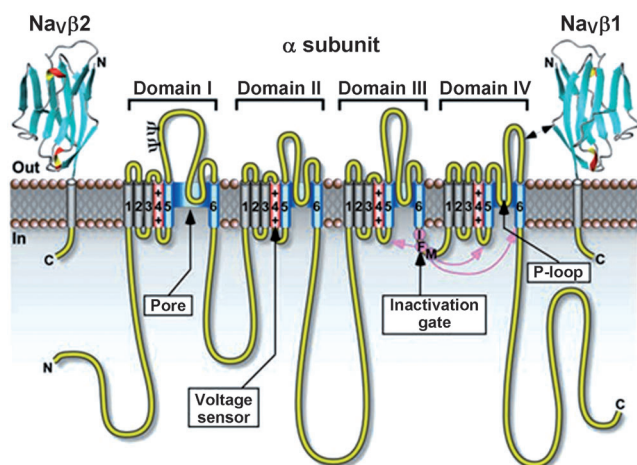

Figure 25. Schematic representation of the molecular structure and membrane topology of Na$_V$. The pore lining α-helices S5 and S6 and the intervening p-loop regions that form the ion conducting pathway are highlighted in blue.[99]

regions connect the four repeats and include sites for protein phosphorylation. Fast inactivation of the channel is mediated by an isoleucine-phenylalanine-methionine (IFM) motif that is located between domains III and IV, and has been proposed to serve as a "hinged lid" to block the inner mouth of the channel pore.[97] In the model by Guy and Seetharamulu, a portion of the sequence between S5 and S6 of each domain folds back into the membrane to create the outer channel mouth and ion selectivity filter.[50,95] This so-called p-loop region is rich in carboxylate residues and has been implicated through mutagenesis and SAR studies to be the guanidinium toxin binding site (Site 1). The narrowest constriction in the conductance pore results from the close-packing of four amino acids (one from each domain) consisting of aspartate (D), glutamate (E), lysine (K), and alanine (A), often referred to as the DEKA loop or selectivity filter.[98] This ring of amino acids forms the base of an outer vestibule of the channel pore where STX and TTX are believed to lodge. Thus, the current picture of guanidinium toxin binding is analogous to a plug that stoppers the opening of a conical hole.

4.2. Critical Amino Acids in the STX Binding Site

Prior to the work of Noda, early insights regarding the pore structure and ion selectivity filter of Na$_V$ were obtained through studies of the relative permeability of organic cations.[100] Findings from these experiments suggested that Na$^+$ conduction occurred through a 3×5 Å wide portal, too narrow to allow for passage of the guanidinium toxins but large enough for guanidinium ion itself.[101] Subsequent investigations by Henderson, Ritchie, and Strichartz demonstrated that monovalent (H$^+$, Li$^+$, Tl$^+$), divalent (Be^{2+}, Mg^{2+}, Ca^{2+}, Sr^{2+}, Ba^{2+}) and trivalent cations (La^{3+}, Sm^{3+}, Er^{3+}) compete with the STX and TTX for a common Na$_V$ binding site.[102,103] These studies led to speculation that the toxin binding site was along the ion permeation pathway. Additional binding experiments using STX and TTX against Na$_V$s modified with functional group-specific reagents revealed further details of the channel pore, suggesting that the selectivity filter is comprised of multiple carboxylate residues (see Figure 29).[30,103a]

cDNA cloning has enabled characterization of the primary amino acid sequences of several eukaryotic Na$_V$ orthologues and subtypes, including those from rat and human brain (Na$_V$1.2),[104] skeletal muscle (Na$_V$1.4),[105] and cardiac myocytes (Na$_V$1.5). Functional expression of most mammalian isoforms and protein mutants is possible in heterologous systems such as frog oocytes or Chinese hamster ovary (CHO) cells. Among the first such experiments were those reported by Noda and co-workers, who demonstrated that replacement of glutamate (E) in the p-loop of repeat I (E387, Na$_V$1.2) with a neutral glutamine (Q) results in > 1000-fold loss in affinity for both STX and TTX.[106] Following this initial disclosure, multiple reports describing extensive mutagenesis experiments against Na$_V$1.2 and 1.4 have appeared.[107] These studies reveal five critical carboxylate residues—D400, E403, E755, E758, D1532 (Na$_V$1.4 numbering)—that are responsible for proper ion conductance and toxin binding. Work by Terlau suggested that these anionic groups cluster in two "rings" as DEKA and EEMD (one amino acid from each repeat in order from I to IV) to form the selectivity filter and outer vestibule loop, respectively (Figure 26).[107]

Alignment of the amino acid sequence of Na$_V$1.4 with evolutionarily-linked voltage-gated Ca^{2+} channels suggested that D400 and E755 together with lysine1237 (K1237) and alanine1529 (A1529) comprise the ion selectivity filter.[108] These four amino acids, DEKA, are conserved throughout all eukaryotic Na$_V$ subtypes; in related Ca$_V$ channels, four glutamates, EEEE, are displayed at structurally homologous sites. Double mutation of the lysine and alanine amino acids in Na$_V$1.2 to glutamates (DEKA→DEEE) profoundly alters ion selectivity, reducing that for Na$^+$ over K$^+$ ($P_K/P_{Na} = 0.03$ for wild-type vs. 0.69 for the lysine to glutamate mutant), while enhancing the permeability of Ca^{2+}.[108] Corresponding mutations to the EEEE ring of the calcium channel further establish the critical role of these amino acid groups for regulating specific ion conductance.[109]

Studies with [^{3}H]-STX and rat cardiac tissue,[110] and subsequently with both STX and TTX on heterologously expressed Na$_V$1.5,[111] established the lack of sensitivity of this
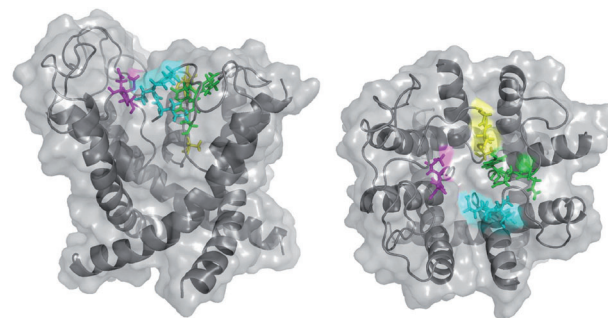
Isoform	Domain I	Domain II	Domain III	Domain IV
Na$_V$1.2	TQDFWEN	CGEWIET	TFKGWMD	TSAGWDG
Na$_V$1.4	TQDYWEN	CGEWIET	TFKGWMD	TSAGWDG
Na$_V$1.5	TQDCWER	CGEWIET	TFKGWMD	TSAGWDG
Na$_V$1.8	TQDSWER	CGEWIEN	TFKGWMD	TSAGWDG

Na$_V$ isoform	Mutation	K_d TTX (nM)	K_d STX (nM)
1.4	None	40	3.0
1.5	None	950	91.1
1.5	C374Y	1.3	5.2
1.5	R377N	7580	184

Figure 26. Top: Alignment of sequences for pore-lining regions of Domain I–IV for Na$_V$1.2, 1.4, 1.5, and 1.8; Bottom: Binding dissociation constants of TTX and STX measured against Na$_V$1.4 and Na$_V$1.5 and select mutants expressed in oocytes.[28]

Species	Domain I	Domain II	Domain III	Domain IV
Fugu[a,64]	QDNWES	GEWIET	FKGWMN	ITTSAG
Clam[b,119]	QDYWEN	GEWIDS	YKGWID	MCTSAG
Garter Snake[c,120]	QDYWEN	GEWIET	FKGWMD	VTTSAG
H.sapiens	QDYWEN	GEWIET	FKGWMD	ITTSAG

Figure 27. A homology model highlighting common sites of pore-lining mutations found in skeletal muscle Na$_V$ of toxin-resistant organisms (green = domain I, cyan = domain II, magenta = domain III, yellow = domain IV); only select examples are given in the table along with the corresponding amino acid sequences for human Na$_V$1.4. Mutations known to destabilize toxin binding are highlighted in blue. Selectivity filter residues, DEKA, are highlighted in red. [a] *Takifugu rupripes.* [b] *Mya arenaria.* [c] *Thamnophis sirtalis.*

channel isoform (ca. 100-fold) towards toxin block. This discovery marks an important historical note in the annals of Na$_V$ research, having inspired considerable research efforts to determine the molecular origin for differences between "TTX-sensitive" and "TTX-insensitive" (such as Na$_V$1.5) subtypes. Defining mutagenesis experiments reveal that differences in toxin binding affinity between Na$_V$ subtypes derive from single amino acid variations in the p-loop region (Figure 26). In Na$_V$1.5, replacement of a cysteine at position 374 (Na$_V$1.5 numbering) with a phenylalanine or tyrosine residue restores nanomolar affinity of TTX and STX.[28] Conversely, destabilization of TTX and STX binding to Na$_V$1.4 occurs when tyrosine 401 (Y401, Na$_V$1.4 numbering) is changed to a cysteine.[112] Analogous toxin IC$_{50}$ measurements have been recorded against wild-type and mutant Na$_V$1.2.[113] The presence of an aromatic amino acid (tyrosine or phenylalanine) in repeat I, one amino acid removed from the selectivity filter, appears to be critical for high affinity toxin block.[114] Two other "TTX-insensitive" isoforms, Na$_V$1.8[115] and 1.9, expressed principally in sensory neurons display a serine (S) residue at this locale. TTX binding studies with mutant Na$_V$s incorporating an unnatural, fluorine-substituted phenylalanine at the 401 position (Na$_V$1.4 numbering) strongly implicate a direct π-cation interaction with the guanidinium group in TTX.[116] Analogous studies with STX have not been described. Absent structural biology, such data provides compelling molecular details of the TTX/STX receptor site.[117]

Gene sequencing of Na$_V$s in organisms known to concentrate TTX and STX (e.g., fugu, clams, garter snakes) gives additional structural insight into the critical contacts between toxin and protein (Figure 27).[64] In fugu skeletal muscle, as in Na$_V$1.5, 1.8, and 1.9, mutation of the aromatic residue at 401 (Na$_V$1.4 numbering) to asparagine (N) confers resistance to toxin block at sub-micromolar concentrations.[118] Other data, including studies with Na$_V$ from *Mya arenaria*, a species of soft-shell clam and a source of STX when harvested during red tides, demonstrate the importance of carboxylate residues for toxin binding.[119] Remarkably, in this example, a single mutation from glutamate (758, Na$_V$1.4 numbering) to aspartate reduces STX affinity by 1500-fold (1.7 vs 2700 nM).

Additional mutations of this sort in organisms resistant to STX and TTX poisoning are likely to be identified with recent advances in gene sequencing techniques.

Although the affinities of TTX and STX for Na$_V$ subtypes are typically within an order of magnitude (which has led to a general assumption that the two toxins are effectively equivalent), studies from multiple labs have identified channel pore-lining mutations that deviate from this norm. A Y401D mutation in Na$_V$1.4 decreases TTX potency by a substantial 4800-fold (IC$_{50}$ = 36 vs. 171 000 nM), but has only a modest influence on STX (55-fold difference, IC$_{50}$ = 3.1 vs 169 nM).[121] Related observations have been made for D384E and W386Y channel mutants.[107] A species-dependent, two-amino acid variation in Na$_V$1.7 has been demonstrated to alter STX affinity by 250-fold in non-primate versus primate orthologues.[122] These structural differences appear in adjacent amino acids in repeat III. Surprisingly, the influence of these two residues on TTX affinity is almost nil (see Section 4.4).

4.3. The Binding of Modified Saxitoxins to Na$_V$ Channels

Binding studies with natural and unnatural derivatives of TTX and STX complement protein mutagenesis experiments for examining the Na$_V$ pore architecture. Measured potencies for channel block by deoxygenated forms of TTX and sulfated STXs (i.e., gonyautoxins) vary from small to substantial in comparison to the parent molecules.[66,123] Among naturally occurring saxitoxin variants (see Figure 5), binding studies with neosaxitoxin (neo-STX), an N1-hydroxylated form of STX, and select gonyautoxins have been particularly infor-

mative. Experiments to measure the ability of neo-STX to inhibit sodium currents in frog skeletal muscle fibers demonstrated that this modification has little influence on toxin potency.[124] The pK_a of the N-OH group in neo-STX has been measured at 6.75; acidity constants for the 7,8,9-guanidine in both STX and neo-STX are 8.25 and 8.65, respectively, and > 11 for the 1,2,3-guanidine in both compounds.[125] At pH values below 8.2, both compounds retain low nanomolar potency against the channel.[126] Only as the pH is increased above pH 8.2 does the affinity of both toxins decline. These results reveal the essential nature of the protonated 7,8,9-guanidine for potent toxin binding and form the basis for toxin-receptor models that position this moiety towards the DEKA loop (selectivity filter).[4,117]

Experiments with C11-α- and β-sulfated toxins, GTX II and GTX III, further support the critical role of the 7,8,9-guanidinium unit for ligand binding.[126–128] Differences in potency for these compounds and structurally allied GTX I and IV relative to STX are modest (e.g., GTX III IC$_{50}$ = 14.9 ± 2.1 nM, rNa$_V$1.4)[122] in spite of the larger volume size and variation in net charge. Accordingly, the dicationic charge of STX is not a prerequisite for high affinity block of the sodium channel.
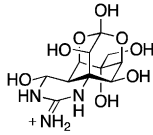
Unnatural derivatives of STX have been prepared through semi-synthesis and include α- and β-saxitoxinol[59,60] as well as C12 oxime adducts.[129] The potency of the former agents (570 ± 30 nM and 33 ± 2 μM against Na$_V$1.4, respectively),[60] is generally cited as evidence against reversible covalent toxin-protein binding.[130] In the aggregate, blocking measurements with these compounds underscore the importance of the hydrated C12-ketone for high affinity toxin block, as the potency of these compounds is significantly reduced compared to STX. Current models for STX binding to the channel pore suggest that the hydrated ketone forms important hydrogen-bond contacts with glutamate 758 (Na$_V$1.4 numbering).[122,131–133] These models, however, do not explain the disparity in IC$_{50}$ values between α- and β-saxitoxinol.

Removal of the C13-carbamate from STX (i.e., dcSTX) can be achieved through acid hydrolysis of the natural product.[134] Excision of this group results in a 12-fold diminution in inhibition of Na$_V$1.4 (earlier studies indicated that dcSTX maintained ca. 1/5 the potency as STX).[135] This modest effect on toxin affinity has prompted efforts to modify the C13-position of STX, which can be achieved in one of two ways: 1) reaction of dcSTX with succinic anhydride to give a C13 ester derivative (albeit in low yield, 16%);[59] 2) de novo synthesis, as exemplified by Du Bois and Nagasawa. The preparation of a N21-dimethyl derivative of STX, by Andresen and Du Bois shows that nitrogen substitution of the carbamate group does not reduce toxin affinity for Na$_V$1.4 (2.1 ± 0.1 nM).[60] Subsequent developments by Llewellyn,[136] Oshima,[137] Nagasawa,[138,139] and Du Bois[60,85–88] have exploited the C13 position of saxitoxin to access modified toxins, including biotin-, affinity- and fluorescently-labeled conjugates (see Sections 5.2, 5.3).
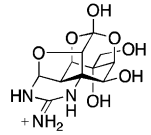
In tandem with studies of STX, electrophysiological measurements and protein binding studies with naturally occurring, deoxygenated forms of TTX have been performed to evaluate the impact of such modifications on toxin binding.[66,140] The structure of TTX and its intrinsic instability to base severely challenge efforts to derivatize the toxin through semi-synthesis.[141] Modification of the C11 alcohol, which includes oxidative C6,C11 cleavage to give the C6-ketone, is possible and has been exploited to prepare a TTX-photoaffinity probe.[142] Protein labeling experiments with this molecule, however, do not reveal specific details of the toxin binding site, as photochemical cross-linking is found to occur at multiple locations.

Among known TTX congeners, 4,9-anhydrotetrodotoxin is arguably the most compelling (Figure 28). This isolate was first identified in 1964 and had been largely dismissed as

Na$_V$ isoform	IC$_{50}$ TTX	IC$_{50}$ 4,9-anhTTX
1.2	7.8 ± 1.3	1260 ± 121
1.3	2.0 ± 0.4	341 ± 36
1.4	4.5 ± 1.0	988 ± 62
1.5	1970 ± 565	78,500 ± 11,600
1.6	3.8 ± 1.5	**7.8 ± 2.3**
1.7	5.5 ± 1.4	1270 ± 251
1.8	1330 ± 459	>30,000

Figure 28. Comparative affinities for TTX and 4,9-anhydroTTX against seven Na$_V$ subtypes, as determined by electrophysiology recordings on *Xenopus* oocytes. The latter compound is found to be a selective inhibitor of Na$_V$1.6.[145]

a weakly potent TTX derivative.[143,144] In 2007, however, Schreibmayer and co-workers disclosed a comprehensive electrophysiological study of 4,9-anhydroTTX against a panel of Na$_V$s comprising seven of the nine mammalian isoforms (Na$_V$1.2–1.8, oocytes).[145] Remarkably, this compound displays unique selectivity for Na$_V$1.6 (IC$_{50}$ = 7.8 nM). By comparison, IC$_{50}$ block of other Na$_V$ subtypes by 4,9-anhydroTTX requires 40–1000 times higher concentrations. While the molecular basis for this differential potency is currently unknown, the ramifications of these data pertaining to the design and development of Na$_V$ isoform-selective inhibitors are potentially profound.

A method that combines both protein mutagenesis and toxin SAR, termed double-mutant cycle analysis, has provided important structural insights into the Na$_V$ toxin receptor site. Studies by Terlau,[107a] Lipkind and Fozzard,[132a] and Dudley[131,146] have led to proposed TTX and STX binding models, the latter of which is depicted in Figure 29. The relative clockwise orientation of the four repeats is based on a best-fit of the mutant-cycle analysis data performed with toxins that include the peptide inhibitor, μ-conotoxin GIIIA.[147] Despite the availability of a large subset of naturally occurring TTX and STX derivatives, structural mapping of the channel through mutant cycle analysis would
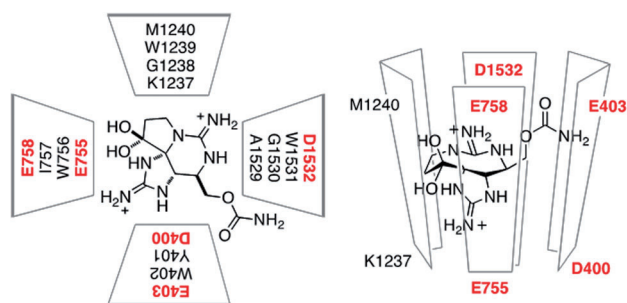
Figure 29. Proposed orientation of STX binding determined by protein mutagenesis, toxin SAR, and double-mutant cycle analysis data. Critical carboxylate residues for high affinity toxin block are highlighted in red.[85]

arguably benefit from the availability of a more diverse collection of toxin analogues—compounds that are accessible through de novo chemical synthesis. Studies that combine protein mutagenesis with compensatory modifications of the toxin structure could lead to the identification of orthogonal toxin/Na$_V$ mutant pairs, potentially enabling tools for chemical genetic studies of Na$_V$ isoform function.

4.4. Computational Na$_V$ Channel Models

Extensive protein mutagenesis and toxin SAR data together with sequence analysis and homology modeling have informed current molecular depictions of the channel pore and toxin binding site. In 1994, prior to the disclosure of even the first cation channel X-ray crystal structure, Lipkind and Fozzard put forth a model of the outer vestibule region of Na$_V$1.4, the most extensively studied channel isoform at the time.[148] The original Lipkind/Fozzard model was comprised of forty amino acids, ten from each of the reentrant loops that connect transmembrane helices S5 and S6 in each repeat. Despite its simplicity by today's standards, the Lipkind/Fozzard model suggested important contacts between carboxylate residues in repeats I and II of the channel (D400, E755, E758, Na$_V$1.4 numbering) with both the 7,8,9-guanidinium ring and C12-hydrated ketone of STX. This view of STX binding also implicated a nonpolar methionine (M1240) in domain III in a hydrophobic interaction with the C10–C11 region of the toxin. The 7,8,9-guandinium ring is positioned towards the narrowest region of the pore, defined by the loop of amino acids, D400-E755-K1237-A1529 (DEKA) that form the ion selectivity filter.

With the availability of the first reported protein X-ray structures of cation channels,[92b] more sophisticated models of the Na$_V$ pore have evolved.[149] A Na$_V$ construct based on KcsA, a homotetrameric, bacterial potassium channel, has been advanced by Lipkind and Fozzard and includes both S5 and S6 helices in addition to the p-loop segments from each repeat.[133] From the X-ray crystallographic analysis of KcsA, an α-helix-turned-β-strand motif was used to template the p-loop segments. Refinement of this model was guided by a series of available reports detailing the contributions of pore-lining amino acid residues to Na$_V$ ion selectivity. Cognizant of mutagenesis studies that designated the lysine

in the DEKA filter as critical for Na$^+$ selectivity, nearest neighbor amino acid contacts with K1237 were evaluated.[98] All told, this sophisticated examination of channel structure has provided the starting point for subsequent investigations of this type.

Alternative computational models of the Na$_V$ pore have been crafted based on MthK, KcsA, and K$_V$AP prokaryotic potassium channel X-ray structures. More recently, Tikhonov and Zhorov[132] have utilized the structure of a bacterial sodium channel, Na$_V$Ab, as a template for analysis of the mammalian orthologue. The former, however, is not blocked by TTX and the degree of structural similarity with the mammalian channel is unclear, as Na$_V$Ab is a homotetramer.[4,50] Reasonable alignment of the Na$_V$1.4 protein sequence with the bacterial channel necessitates the introduction of a one-residue gap in the p-loop region. This adjustment reconciles the side chain orientation of key amino acids known to contact TTX. Despite impressive advances over the past two decades in protein structure prediction, accurate modeling of the secondary and tertiary structure of a protein the size and complexity of the Na$_V$ α-subunit remains an inexact science.

A molecular model of the Na$_V$ pore fabricated from the structure of K$_V$AP (Figure 30) has been used to rationalize differences in STX, GTX III, and TTX potency towards the
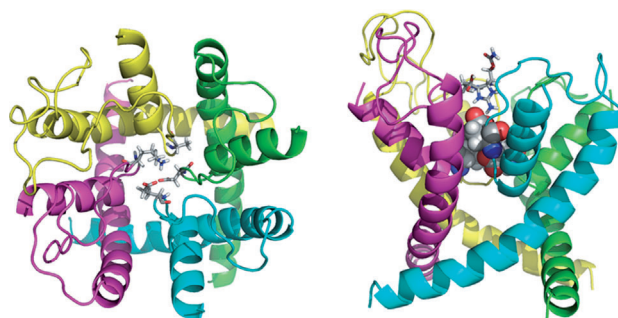

Figure 30. A rNa$_V$1.4 homology model[122] displaying the S6 and p-loop residues, as viewed from the extracellular side (left) and from the membrane (right). The four domains of the pore are colored green (domain I), cyan (domain II), magenta (domain III), and yellow (domain IV). Residues comprising the DEKA selectivity filter are displayed as stick and space-filling models; atoms are colored red (oxygen), blue (nitrogen), white (hydrogen), gray (carbon). STX binds above the selectivity filter, as shown in the side view.

human Na$_V$1.7 subtype (see Section 4.3).[122] The disclosure by Walker, et al challenges a long-accepted view that STX and TTX have similar affinity profiles against the nine mammalian "toxin-sensitive" and "toxin-insensitive" Na$_V$ isoforms (Table 2).[122] Electrophysiological recordings on the α-subunit of hNa$_V$1.7 expressed in CHO cells expose marked differences in potencies between STX, GTX III, and TTX. Concentration–response curves give IC$_{50}$ values of 702 and 1513 nM for STX and GTX III, respectively, while block of this channel by TTX reaches 50% at 19 nM concentrations. These data contrast the measured potencies of the three toxins for inhibition of Na$_V$1.4, for which IC$_{50}$ data are all within an order of magnitude. Sequence alignment of Na$_V$1.4 and 1.7 reveals two amino acid differences in structurally

Na$_V$ isoform	Mutation	IC$_{50}$ TTX	IC$_{50}$ STX
1.4	none	17.1 ± 1.2	2.8 ± 0.1
1.4	M1240T	466 ± 42	73 ± 2.6
1.4	D1241I	8.7 ± 0.8	53 ± 4.6
1.4	M1240T, D1241I	90 ± 4.7	1153 ± 60
1.7	none	18.6 ± 1.0	702 ± 53
1.7	T1398M, I1399D	5.0 ± 0.9	2.3 ± 0.2

homologous sites of domain III in the p-loop region (M1240, D1241 in Na$_V$1.4; T1398, I1399 in Na$_V$1.7). This double variation appears only in Na$_V$1.7 and, rather remarkably, only in primate orthologues. Single and double point amino acid mutation together with toxin binding studies confirm that these two residues are directly responsible for altering the STX/TTX selectivity profile.

Molecular modeling and ligand docking studies suggest that the MD→TI variation between Na$_V$1.4 and 1.7 significantly alters the local electrostatic potential surface and volume size of the outer vestibule (Figure 31).[122] Binding of STX to hNa$_V$1.7 is presumably destabilized due to a reduction in Coulombic attraction and a loss of close-packing between ligand and receptor because of the large void space created by threonine and isoleucine substitution. Differences in TTX and STX affinity to hNa$_V$1.7 manifest largely as a result of the very different charge surfaces between these two compounds. At the limits of the current model, these findings raise the tantalizing possibility that a STX derivative could be crafted as a selective inhibitor of hNa$_V$1.7. Given the intense interest in this protein target for pain research, such a discovery could have significant translational impact.[48]

Computational advances together with the near certainty that structural biology will someday provide atomic resolution of a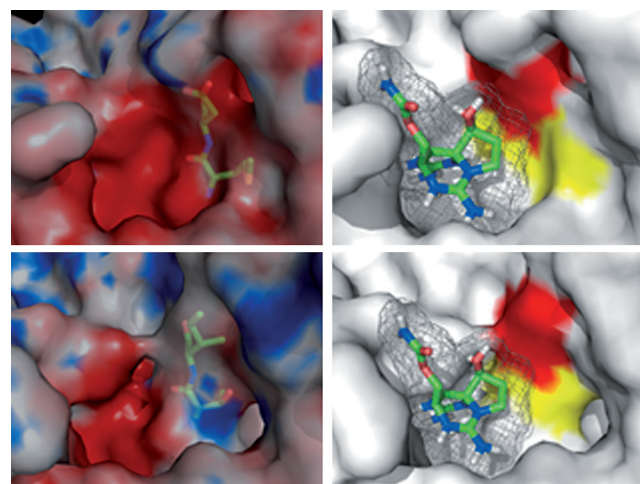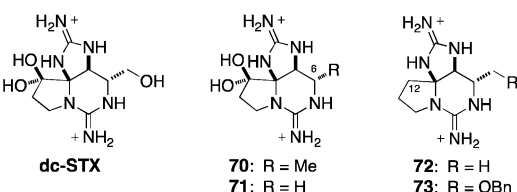 mammalian Na$_V$ channel will further shape our understanding of toxin binding. The intrinsic dynamic nature of voltage-gated ion channels requires that proteins rapidly cycle through different conformational states (grossly considered as open, inactivated, and closed).[2b] Accordingly, protein mutagenesis and toxin SAR data will continue to augment our understanding of Na$_V$ structure even if/when specific protein conformers are revealed by X-ray crystallography. As of this moment, available models of the outer mouth and selectivity filter of Na$_V$ are unable to explain specific phenomenology, including differences in toxin affinity between different isoforms (e.g., channels expressed in fugu, clam, garter snake) and the differential potencies of closely related toxin compounds (e.g., α- and β-saxitoxinols, TTX and 4,9-anhydroTTX). In due course, answers to such questions will be unveiled, and with access to new toxin derivatives through chemical synthesis, the rational design of potent Na$_V$ subtype specific inhibitors may be realized.

5. Molecular Probes for Na$_V$ Studies

Interest in Na$_V$ structure/function, the uniqueness of STX as a Na$_V$-selective inhibitor, and the ability to access this molecule through chemical synthesis inspire efforts to design toxin analogues for biochemical and pharmacological studies. Such agents have potential utility for mapping details of the pore architecture and challenging the accuracy of homology models, as probes for marking the cellular location of Na$_V$s and for elucidating the physiological role of individual Na$_V$ isoforms, and as next-generation therapeutics for treatment of pain. With regard to the latter possibility, reports of human clinical data have demonstrated the effectiveness of STX,[150] GTX,[151] and neo-STX[152] as long-acting, local anesthetics for chronic and neuropathic pain, though systemic toxicity remains a significant concern. The desire for subtype-specific modulators of Na$_V$, as clinically safe and effective analgesics that target isoforms believed responsible for nociception (Na$_V$1.3, 1.6, 1.7, 1.8), poses a formidable challenge in drug discovery.[48] Topological differences in the p-loop region of Na$_V$ isoforms—as noted by the recent identification of 4,9-anhydroTTX as a Na$_V$1.6 selective blocker, the differential influence of amino acid mutations on toxin binding, and the discovery of natural amino acid variations in human Na$_V$1.7 that distinguish this isoform from others—raise the intriguing possibility that a modified STX could be engineered to target a single channel subtype. The pursuit of such an idea starting from a lead as complex as STX is only possible with the power of modern chemical synthesis.

5.1. Kishi/Strichartz

Kishi's disclosure of the total synthesis of (±)-STX enabled subsequent evaluation of a select number of derivative structures, including both antipodes of dcSTX and unnatural C12 and C13-deoxy-forms (Figure 32). Studies in collaboration with Strichartz to determine binding affinities included competitive displacement assays using tritiated STX ([³H]-STX) against channels expressed in rabbit brain.[153] In

Figure 31. Homology model[122] derived images showing differences between Na$_V$1.4 (top) and Na$_V$1.7 (bottom). Figures on the right show STX docked in identical poses to highlight the steric differences of the two point M→T, D→I variation. M1240 and T1398 are colored in yellow and D1241 and I1399 in red.

Figure 32. Binding dissociation constants (K_i) and differential potencies (EC_{50}) for C6 and C12-modified saxitoxins.[153] Data obtained from analysis of compound action potential (AP) inhibition in desheathed sciatic nerves of *Rana pipiens*.[154]

Compound	K_i (M x 10^{-9})	$K_{i(STX)}/K_i$	EC_{50} (nM)
(+)-STX	0.96 ± 0.07	1	7.2 ± 1.3
(+)-dcSTX	3.80 ± 0.68	0.25	16 ± 3
(−)-dcSTX	33.9 ± 3.6	0.03	30 ± 6
70	960 ± 15	10^{-3}	2.3 ± 0.6 x 10^3
71	3.5 ± 0.4 x 10^4	2.8 x 10^{-5}	2.5 ± 0.5 x 10^5
72	ND	ND	7.7 ± 1.0 x 10^5
73	5.9 ± 2.4 x 10^5	1.6 x 10^{-6}	>10^6

these experiments, the inhibitory dissociation constant (K_i) of (+)-dcSTX, the natural enantiomer, was measured at 3.8 nM ((+)-STX K_i = 0.96 nM). Single channel electrophysiological recordings confirm that (+)-dc-STX is 25–40% less potent than the natural product. Surprisingly, (−)-dcSTX showed measurable blocking activity, but this result is ascribed to a 3–4% contamination of the sample with the (+)-isomer. Removal of either the C13-alcohol (**70**, doSTX) or the C13 substituent altogether (**71**) results in a substantial diminution in ligand-receptor binding, as does deoxygenation of the C12 carbon (**72**, **73**).

Collectively, these binding studies with STX analogues confirm that protein interaction with the C13-carbamate group does not play a significant role in toxin binding. In addition, these data demonstrate that toxin binding is stereoselective, thus justifying the development of new routes to STX that can deliver the product in optically pure form.

5.2. Yotsu-Yamashita/Nagasawa

A recent disclosure by Nagasawa offers a systematic analysis of the inhibitory activities of three C13-modifed STXs and three related fused-tricyclic structures, referred to as FD-STXs.[138] All six compounds are available through total synthesis as single enantiomers. FD-STXs are prepared from alcohol **74**, which gives hemi-aminal **75** upon treatment with IBX (Figure 33). Using this protocol, three unique structures—FD-C13-deoxy-STX (FD-doSTX, **76**), FD-C13-decarbamoyl-STX (FD-dcSTX, **77**), and FD-STX (**78**)—have been obtained (Figure 33).

Binding affinities to Na_V for both STX and FD-STX derivatives were evaluated using a cell-viability assay with Neuro-2A cells[155] and by whole-cell voltage-clamp electrophysiology (HEK293 cells). The latter experiments were performed with recombinant $Na_V1.4$ and 1.5 to examine differences in subtype potency. While FD-STXs are ca.
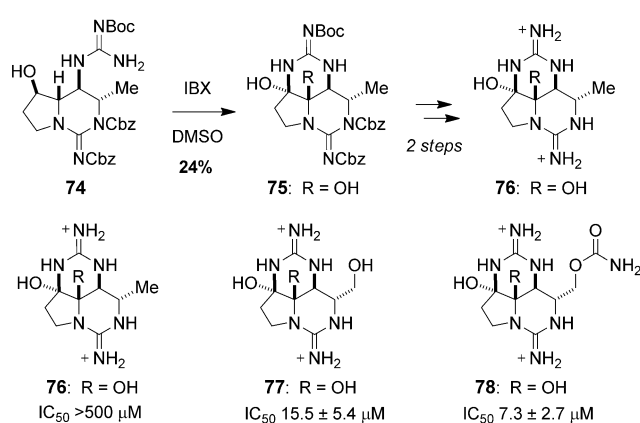

Figure 33. Isomeric forms of STX display diminished potency against Na_V in Neuro-2a cells.

1000 times less potent than analogous STX derivatives, like these natural toxins, FD-STX and FD-dcSTX display preferential affinity for $Na_V1.4$ over 1.5. Furthermore, as with previous comparative studies of STX, dcSTX, and doSTX, the relative loss in potency for FD-STX and C13-derivatives follows a similar trend (i.e., FD-dcSTX is less potent than FD-STX). Against $Na_V1.5$, FD-dcSTX shows surprising irreversible inhibition of ion conduction. A mechanistic rationale for this intriguing observation that accounts for differences between FD-STX and the decarbamoylated derivative awaits further experimentation.

The demonstration that FD-STX derivatives can block channel function at low micromolar concentrations is reminiscent of findings by Gawley, who showed that a STX-inspired mono-guanidine derivative can also act as an inhibitor of $Na_V1.1$ and 1.2 (rat neuronal B50 cells).[156] These data, when considered alongside the fact that STX and other PSPs, TTX, and ZTX are all effective at occluding the outer pore, suggest that Site I is a rather promiscuous receptor for organic cations. Findings from protein mutagenesis studies, however, argue in favor of a "rigid" pore architecture (see Section 4.2). Resolving these apparent structural discrepancies merits additional mutagenesis experiments and SAR studies with toxin analogues.

The Nagasawa route to (+)-STX can be modified at an intermediate stage to enable selective incorporation of a C13-azido group **79** (Figure 34). From this compound, three unique STX derivatives bearing acetamide **80**, urea **81**, and guanidine **82** groups at C13 have been assembled. Using a Neuro2a[155] cell-based assay, which gives an IC_{50} for (+)-dcSTX of 4.4 nM, the measured potencies for **80**, **81**, and **82** are found to be 1000-, 20-, and 50-times less than that of dcSTX.[139] A rationalization for these data posits the
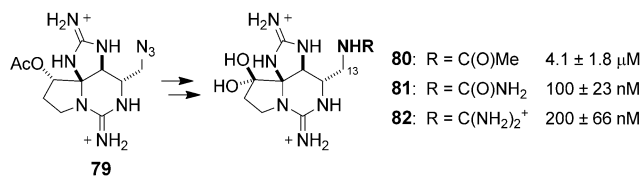

Figure 34. IC_{50} values for C13-carboxamide, urea, and guanidinium analogues of STX.

influence of both hydrophilicity and charge balance on inhibitor binding.

5.3. Du Bois

Dynamic changes in Na_V subtype expression, localization, voltage responsiveness, and ion conduction all contribute to shape the amplitude and frequency of action potentials. The existence of nine gene loci that encode nine unique Na_V α-subunits in mammalian cells belies the heterogeneity in membrane protein structure introduced through RNA splicing, RNA editing, and posttranslational modifications (PTMs, e.g., glycosylation, phosphorylation, methylation).[157] Efforts to prepare modified saxitoxins are guided by a desire to understand how changes to Na_V structure, including PTMs, and subtype expression levels influence action potential outputs and, ultimately, behavioral response.

Investigations by Du Bois and co-workers have given way to a number of novel carbamate-modified STX derivatives, including fluorescent, affinity, and radiolabeled conjugates.[60, 84–87, 158] These compounds are intended for live cell and animal imaging of Na_Vs and for protein isolation and characterization studies. The rapid and reversible binding of the guanidinium toxins to the outer mouth of the channel distinguishes these compounds from other known small molecule modulators of Na_Vs (e.g., steroidal alkaloids, pyrethrins, ladder toxins, local anesthetics).[159] This characteristic, along with the fact that the N21 position of the toxin can be modified without significantly disrupting binding affinity, favors STX as a starting point for the development of Na_V probes for cellular imaging.

Assembly of N21-modified STX derivatives is made possible through adaptation of Du Bois' previously published route to (+)-STX.[85] Oxazolidinone **83** is central to the design of this plan, as reaction of this intermediate with either a primary or secondary amine introduces the desired N21 substituent (Figure 35). The electrophilic reactivity of the oxazolidinone is ascribed to the inductive effect of the N-guanidinyl group and the torsional strain of the fused six-membered ring. Completion of each toxin derivative is accomplished in two steps from **84** through Lewis acid mediated guanidine cyclization/deprotection and C12-alcohol oxidation.

Potency measurements of a small set of N21-toxin derivatives give insight into the structural limitations of carbamate substitution. Straight chain saturated alkyl groups (*n*-heptyl, **85**) increase IC_{50} 10-fold from that of (+)-STX (measured against Na_V1.4, CHO cells). Branched alkyl groups such as isopropyl or cyclohexyl (**86**) diminish toxin affinity to a greater extent, suggesting that the carbamate group lies within a narrow space, perhaps between subunit domains. The influence of charged and polar functional groups on toxin derivative binding is also illustrated by these data.[60, 85]
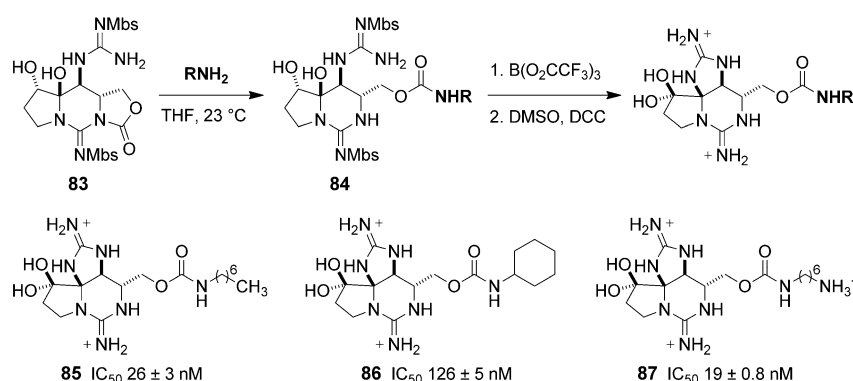

Figure 35. A general pathway for preparing carbamoyl derivatives of STX. Select analogues are shown with IC_{50} values determined by electrophysiology recordings against Na_V1.4 in CHO.[60, 85, 86]

N21-Hexylamine **87**, and related ethyl, propyl, butyl, and octyl structures, have been invaluable starting materials for the preparation of toxin conjugates. Under slightly alkali conditions (pH 8.5–9.5), selective amide formation with **87** and a reactive *N*-hydroxysuccinimide (NHS)-based ester is possible. Yields for this process can range from 30–60 % depending on the structure of the electrophilic group. Using this type of ligation strategy, fluorescent reporter groups and cysteine-reactive maleimide derivatives have been successfully conjoined to the toxin core. This same type of coupling procedure can be employed with *p*-^{18}F-benzoic acid NHS ester to generate a labeled toxin for autoradiography and positron-emission tomography (PET) experiments.[158]

Information on the dynamics of Na_Vs within the cell membrane can, in principle, be obtained using Na_Vs fused to fluorescent proteins (i.e., GFP);[160] such labeling methods, however, are hampered by poor protein expression levels and/or problems with protein trafficking.[161] Immunostaining of Na_Vs in cells or tissues utilizing labeled antibodies is an extremely powerful method for marking protein locations, but cells must be fixed in order for these agents to permeate the cell membrane. Toxin-dye conjugates thus offer unique imaging tools for real-time, live cell tracking of Na_V distributions.

Live cell imaging of Na_Vs has been demonstrated using first generation fluorescent STXs, **88** and **89** (Figure 36). Electrophysiology recordings against differentiated PC12 cells, a neuronal cell model that expresses rNa_V1.2 and 1.7, establish that these compounds retain low nanomolar potency as channel blockers despite the attachment of a large, lipophilic dye. Localization of the dye molecules to the somatic membrane and in neuritic processes is observed in confocal microscopy images, and is consistent with previous studies to mark the spatial locations of Na_Vs in PC12 cells. These data also confirm that fluorescence is restricted to the outer membrane.

The application of **88** and **89** for live-cell, single molecule and super-resolution imaging of Na_Vs reveal fine details of the cell structure and give information about the motility of channels in different cellular regions.[87] Visualization of single channels in the soma, neurites, and neurite projections allows for pointillist reconstruction of the entire cell body. Highly
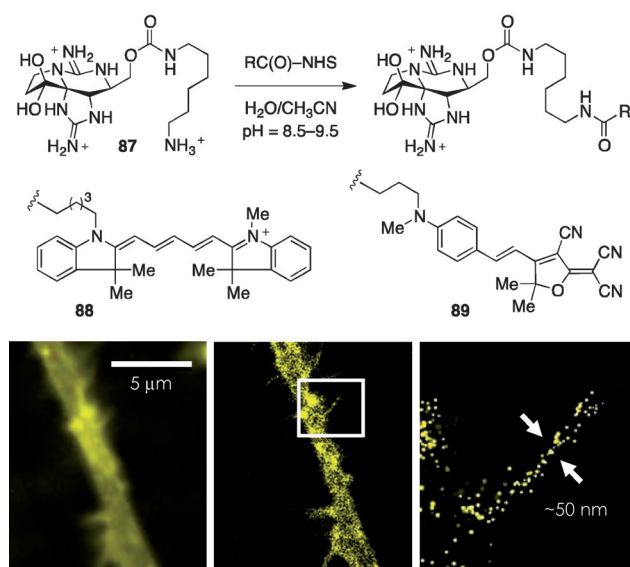
Figure 36. Modified saxitoxins for wide-field fluorescence (left) and superresolution imaging (middle, right). Images are of a neuritic shaft (left, middle) and spine (right) obtained on PC12 cells treated with nerve-growth factor.[87]

Figure 38. Synthesis of a radiolabeled PET tracer through selective conjugation with STX-hexylamine **86**.[158] RCY = radiochemical yield.

The availability of STX conjugates containing either fluorescent reporter groups and/or reactive electrophiles should empower subsequent investigations aimed at tracking Na_V populations and identifying subtype distributions in cells and tissue. Ultimately, molecular probes, such as a radiolabeled [^{18}F]-STX (**91**, Figure 38), may allow for in vivo, serial monitoring of aberrant changes in Na_V expression linked to genetic or environmental factors or in response to therapeutic treatments.[158]

6. Conclusion

The venerable history of STX now spans more than 80 years, its value as a chemical tool in neuroscience, along with its counterpart TTX, having been captured on the pages of textbooks. Among other disciplines, interest in STX crosses chemical synthesis, chemical biology, pharmacology, and public health. These structurally unique, secondary metabolites of unicellular organisms act as acute poisons by shutting down electrical signaling in neuronal cells through selective, high affinity block of voltage-gated sodium channels. Our current understanding of channel structure, protein subtype expression and spatial distributions in cells has been largely informed through studies with these molecules.

Interest in STX shows no sign of waning, particularly now that this molecule, related gonyautoxins, and analogue forms can be prepared efficiently through chemical synthesis. Pharmacological investigations of STX and its natural congeners have been prompted by human patient data that correlates severe pathologies with Na_V malfunction, among which pain sensation is arguably foremost.[150–152, 162] Chemical synthesis can deliver novel STX derivatives for such investigations, as well as chemical probes for structure–activity studies, protein labeling in live cells, protein purification and characterization. With the recognition that 4,9-anhydroTTX selectively blocks Na_V1.6 function and that natural variations in the pore-loop region of the channel alter the relative affinities of the guanidinium toxins for Na_V1.7, the outer pore appears to be a viable locus around which to target Na_V subtype specific inhibitors. The identification of modified saxitoxins that block single Na_V isoforms may indeed prove feasible.

Absent crystal structures of mammalian Na_Vs, molecular models of the channel pore and selectivity filter—to aid both

fluxional lateral movements, extensions, and retractions of filopodia can be captured in quasi-real-time movies and the rates of these processes determined. Single particle tracking experiments and instantaneous velocity measurements characterize the dynamics of Na_Vs and expose differences in the speeds with which channels traverse the cell membrane.

N21-Saxitoxin derivatives possessing a cysteine-reactive maleimide are available through NHS-conjugation chemistry with starting materials such as **87**. Binding of these compounds to wild-type Na_Vs expressed in CHO cells (Na_V1.2, 1.4) and endogenous channel proteins found in rat hippocampal neurons is found to be irreversible, consistent with covalent protein modification (Figure 37). A series of control experiments supports a mechanism in which toxin binding precedes maleimide alkylation of a proximal amino acid residue. With the availability of bifunctional toxin conjugates containing both a reactive electrophile and a functional group for selective ligation chemistries (e.g., ketone as in **90**), Na_V labeling with fluorescent markers or protein cofactors (biotin) should be possible. Such probes could enable tracking of channel endocytosis or facilitate isolation and identification of Na_Vs expressed at the cell surface.
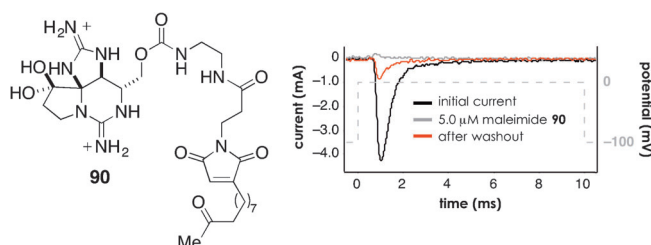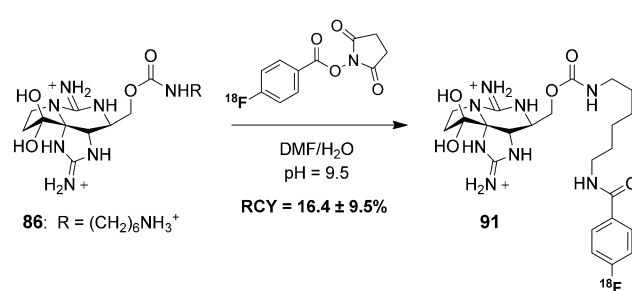

Figure 37. Maleimide conjugates of STX act as irreversible inhibitors of STX-sensitive, wild type Na_V (data shown from experiments on Na_V1.2).[88]

chemical probe and therapeutic design—have been rendered through a combination of protein sequencing and SAR data with toxin congeners and protein mutants. Future investigations of Na$_V$ structure can now capitalize on de novo toxin production, in combination with modern methods of molecular biology and electrophysiology for analyzing Na$_V$s in heterologous expression systems, to further refine our view of the channel pore architecture. Against the backdrop of these investigations is an unmet need for new chemical tools to facilitate studies aimed at understanding the diverse and complex role of Na$_V$s in cell signaling processes and the underlying molecular mechanisms of Na$_V$-related disorders. To this end, Nature, it seems, has provided an extraordinary "lead compound" in saxitoxin.

[1] a) *Tetrodotoxin, Saxitoxin, and the Molecular Biology of the Sodium Channel, Vol. 479* (Eds.: C. Y. Kao, S. R. Levinson), Annals of the New York Academy of Science, New York, **1986**; b) W. A. Catterall, A. L. Goldin, S. G. Waxman, *Pharmacol. Rev.* **2005**, *57*, 397–409; c) T. Narahashi, *J. Toxicol. Toxin Rev.* **2001**, *20*, 67–84.

[2] a) B. Hille, *Ion Channels of Excitable Membranes, 3rd ed.*, Sinauer Associates, Sunderland, **2001**; b) W. A. Catterall, *J. Physiol.* **2012**, *590*, 2577–2589.

[3] T. Narahashi, *Proc. Jpn. Acad. Ser. B* **2008**, *84*, 147–154.

[4] For recent reviews on tetrodotoxin, see: a) T. Nishikawa, M. Isobe, *Chem. Rec.* **2013**, *13*, 286–302; b) E. G. Moczydlowski, *Toxicon* **2013**, *63*, 165–183.

[5] For a recent journal special issue on tetrodotoxin, see: *Mar. Drugs* **2010**, *8*(2), 219–339 (Ed.: P. Ruben).

[6] C. H. Lee, P. C. Ruben, *Channels* **2008**, *2*, 407–412.

[7] a) L. E. Llewellyn, *Nat. Prod. Rep.* **2006**, *23*, 200–222; b) K. D. Cusick, G. S. Sayler, *Mar. Drugs* **2013**, *11*, 991–1018.

[8] T. Narahashi, J. W. Moore, W. R. Scott, *J. Gen. Physiol.* **1964**, *47*, 965–974.

[9] a) B. Hille, *J. Gen. Physiol.* **1971**, *58*, 599–619; b) B. Hille, *J. Gen. Physiol.* **1972**, *59*, 637–658; c) B. Hille, *J. Gen. Physiol.* **1975**, *66*, 535–560; d) C. M. Armstrong, *J. Gen. Physiol.* **1971**, *58*, 413–437; e) C. M. Armstrong, F. Bezanilla, *Nature* **1973**, *242*, 459–461; f) C. M. Armstrong, F. Bezanilla, E. Rojas, *J. Gen. Physiol.* **1973**, *62*, 375–391.

[10] a) A. L. Hodgkin, A. F. Huxley, *J. Physiol.* **1952**, *116*, 424–448; b) A. L. Hodgkin, A. F. Huxley, *J. Physiol.* **1952**, *116*, 449–472; c) A. L. Hodgkin, A. F. Huxley, *J. Physiol.* **1952**, *116*, 473–496; d) A. L. Hodgkin, A. F. Huxley, *J. Physiol.* **1952**, *116*, 497–506; e) A. L. Hodgkin, A. F. Huxley, *J. Physiol.* **1952**, *117*, 500–544.

[11] C. Y. Kao, A. Nishiyama, *J. Physiol.* **1965**, *180*, 50–66.

[12] M. H. Evans, *Br. J. Pharmacol.* **1964**, *22*, 478–485.

[13] STX is known to bind to targets other than Na$_V$, albeit with lower affinity. Interested readers are encouraged to consult reference [7].

[14] T. Narahashi, *Physiol. Rev.* **1974**, *54*, 813–889.

[15] a) F. A. Fuhrman, G. J. Fuhrman, H. S. Mosher, *Science* **1969**, *165*, 1376–1377; b) J. Shindelman, H. S. Mosher, F. A. Fuhrman, *Toxicon* **1969**, *7*, 315–319; c) Y. H. Kim, G. B. Brown, H. S. Mosher, F. A. Fuhrman, *Science* **1975**, *189*, 151–152; d) G. B. Brown, Y. H. Kim, H. Küntzel, H. S. Mosher, G. J. Fuhrman, F. A. Fuhrman, *Toxicon* **1977**, *15*, 115–128; e) M. Yotsu-Yamashita, Y. H. Kim, S. C. Dudley, Jr., G. Choudhary, A. Pfahnl, Y. Oshima, J. W. Daly, *Proc. Natl. Acad. Sci. USA* **2004**, *101*, 4346–4351.

[16] For reviews on STX and related PSPs, see: a) M. Wiese, P. M. D'Agostino, T. Mihali, M. C. Moffitt, B. A. Neilan, *Mar. Drugs* **2010**, *8*, 2185–2211; b) G. Blunden, *Phytother. Res.* **2001**, *15*, 89–94; c) R. F. Clark, S. R. Williams, S. P. Nordt, A. S. Manoguerra, *Undersea Hyperbaric Med.* **1999**, *26*, 175–184.

[17] a) C. Y. Kao in *Algal Toxins in Seafood and Drinking Water* (Ed.: I. R. Falkoner), Academic Press, New York, **1993**, pp. 75–86; b) L. Lehane, *Paralytic Shellfish Poisioning: A Review*, National Office of Animal and Plant Health, Agriculture, Fisheries, and Forestry, Canberra, **2000**.

[18] H. Holmberg, *Holmbergs ethnographic sketches, The Ramuson Library Historical Translation Series, Vol. 1* (Eds.: F. Jaensch, M. W. Falk), University of Alaska Press, Fairbanks, **1985**.

[19] Recent evidence suggests that STX and related toxins are produced exclusively in Nature by cyanobacteria and dinoflagellates and are subsequently concentrated by various organisms. For a recent review on the evolution of STX synthesis in cyanobacteria and dinoflagellates, see ref. [63].

[20] a) H. Sommer, *Science* **1932**, *76*, 574–575; b) M. Prinzmetal, H. Sommer, C. D. Leake, *J. Pharmacol. Exp. Ther.* **1932**, *46*, 63–74; c) H. Sommer, K. F. Meyer, *AMA Arch. Pathol.* **1937**, *24*, 560–598; d) H. Sommer, W. F. Whedon, F. A. Kofoid, R. Stohler, *AMA Arch. Pathol.* **1937**, *24*, 537–559.

[21] a) E. J. Schantz, J. D. Mold, D. W. Stanger, J. Shavel, F. J. Riel, J. P. Bowden, J. M. Lynch, R. S. Wyler, B. Riegel, H. Sommer, *J. Am. Chem. Soc.* **1957**, *79*, 5230–5235; b) J. D. Mold, J. P. Bowden, D. W. Stanger, J. E. Maurer, J. M. Lynch, R. S. Wyler, E. J. Schantz, B. Riegel, *J. Am. Chem. Soc.* **1957**, *79*, 5235–5238.

[22] E. J. Schantz, *Environ. Lett.* **1975**, *9*, 225–237.

[23] R. RaLonde, *Alaska's Mar. Resources* **1996**, *8*, 1–7.

[24] W. J. Brackenbury, L. L. Isom, *Front. Pharmacol.* **2011**, *2*, 53.

[25] For representative literature, see: a) A. Schroeter, S. Walzik, S. Blechschmidt, V. Haufe, K. Benndorf, T. Zimmer, *J. Mol. Cell. Cardiol.* **2010**, *49*, 16–24; b) R. Numann, W. A. Catterall, T. Scheuer, *Science* **1991**, *254*, 115–118; c) J. W. Schmidt, W. A. Catterall, *J. Biol. Chem.* **1987**, *262*, 13713–13723; d) P. Beltran-Alvarez, S. Pagans, R. Brugada, *J. Proteome Res.* **2011**, *10*, 3712–3719.

[26] Ref. [1b].

[27] W. A. Catterall, *J. Physiol.* **2012**, *590*, 2577–2589.

[28] J. Satin, J. W. Kyle, M. Chen, P. Bell, L. L. Cribbs, H. A. Fozzard, R. B. Rogart, *Science* **1992**, *256*, 1202–1205.

[29] J. J. Clare, S. N. Tate, M. Nobbs, M. A. Romanos, *Drug Discovery Today* **2000**, *5*, 506–520.

[30] P. Schrager, C. Profera, *Biochim. Biophys. Acta* **1973**, *318*, 141–146.

[31] M. Nakamura, T. Yasumoto, *Toxicon* **1985**, *23*, 271–276.

[32] Y. H. Chen, T. J. Dale, M. A. Romanos, W. R. Whitaker, X. M. Xie, J. J. Clare, *Eur. J. Neurosci.* **2000**, *12*, 4281–4289.

[33] M. Chahine, P. B. Bennett, A. L. George, Jr., R. Horn, *Pfluegers Arch.* **1994**, *427*, 136–142.

[34] P. S. Dietrich, J. G. McGivern, S. G. Delgado, B. D. Koch, R. M. Eglen, J. C. Hunter, L. Sangameswaran, *J. Neurochem.* **1998**, *70*, 2262–2272.

[35] L. Sangameswaran, L. M. Fish, B. D. Koch, D. K. Rabert, S. G. Delgado, M. Ilnikca, L. B. Jakeman, S. Novakovic, K. Wong, P. Sze, E. Tzoumaka, G. R. Stewart, R. C. Herman, H. Chang, R. M. Eglen, J. C. Hunter, *J. Biol. Chem.* **1997**, *272*, 14805 – 14809.

[36] A. N. Akopian, L. Sivilotti, J. N. Wood, *Nature* **1996**, *379*, 257 – 262.

[37] T. R. Cummins, S. D. Dib-Hajj, J. A. Black, A. N. Akopian, J. N. Wood, S. G. Waxman, *J. Neurosci.* **1999**, *19*, 1 – 6.

[38] A. N. Akopian, V. Souslova, S. England, K. Okuse, N. Ogata, J. Ure, A. Smith, B. J. Kerr, S. B. McMahon, S. Boyce, R. Hill, L. C. Stanfa, A. H. Dickenson, J. N. Wood, *Nat. Neurosci.* **1999**, *2*, 541 – 548, and references therein.

[39] T. R. Cummins, P. L. Sheets, S. G. Waxman, *Pain* **2007**, *131*, 243 – 257.

[40] a) M. H. Meisler, J. E. O'Brien, L. M. Sharkey, *J. Physiol.* **2010**, *588*, 1841 – 1848; b) M. H. Meisler, J. A. Kearney, *J. Clin. Invest.* **2005**, *115*, 2010 – 2017.

[41] A. S. Amin, A. Asghari-Roodsari, H. L. Tan, *Pfluegers Arch. Eur. J. Physiol.* **2010**, *460*, 223 – 237.

[42] G. C. Ebers, A. L. George, Jr., R. L. Barchi, S. S. Ting-Passador, R. G. Kallen, G. M. Lathrop, J. S. Beckmann, A. F. Hahn, W. F. Brown, R. D. Campbell, A. J. Hudson, *Ann. Neurol.* **1991**, *30*, 810 – 816.

[43] A. L. George, Jr., *J. Clin. Invest.* **2005**, *115*, 1990 – 1999.

[44] a) P. L. Sheets, J. O. Jackson, Jr., S. G. Waxman, S. D. Dib-Hajj, T. R. Cummins, *J. Physiol.* **2007**, *581*, 1019 – 1031; b) Y. Yang, Y. Wang, S. Li, Z. Xu, H. Li, L. Ma, J. Fan, D. Bu, B. Liu, Z. Fan, G. Wu, J. Jin, B. Ding, X. Zhu, Y. Shen, *J. Med. Genet.* **2004**, *41*, 171 – 174; c) T. R. Cummins, S. D. Dib-Hajj, S. G. Waxman, *J. Neurosci.* **2004**, *24*, 8232 – 8236.

[45] a) C. R. Fertleman, C. D. Feerrie, J. Aicardi, N. A. F. Bednarek, E. Eeg-Olofsson, F. V. Eimslie, D. A. Griesemer, F. Goutlères, M. Kirkpatrick, N. O. Malmros, M. Pollitzer, M. Rossiter, E. Roulet-Perez, R. Schubert, V. V. Smith, H. Tessard, V. Wong, J. B. P. Stephenson, *Neurology* **2007**, *69*, 586 – 595; b) C. R. Fertleman, M. D. Baker, K. A. Parker, S. Moffatt, F. V. Eimslie, B. Abrahamsen, J. Ostman, N. Klugbauer, J. N. Wood, R. M. Gardiner, M. Rees, *Neuron* **2006**, *52*, 767 – 774.

[46] a) J. J. Cox, J. Sheynin, Z. Shorer, F. Reimann, A. K. Nicholas, L. Zubovic, M. Baralle, E. Wraige, E. Manor, J. Levy, C. G. Woods, R. Parvari, *Hum. Mutat.* **2010**, *31*, E1670 – E1686; b) K. B. Nilsen, A. K. Nicholas, C. G. Woods, S. I. Mellgren, M. Nebuchennykh, J. Aasly, *Pain* **2009**, *143*, 155 – 158; c) Y. P. Goldberg, J. MacFarlane, M. L. MacDonald, J. Thompson, M. P. Dube, M. Mattice, R. Fraser, C. Young, S. Hossain, T. Pape, B. Payne, C. Radomski, G. Donaldson, E. Ives, J. Cox, H. B. Younghusband, R. Green, A. Duff, E. Boltshauser, G. A. Grinspan, J. H. Dimon, B. G. Sibley, G. Andria, E. Toscano, J. Kerdraon, D. Bowsher, S. N. Pimstone, M. E. Samuels, R. Sherrington, M. R. Hayden, *Clin. Genet.* **2007**, *71*, 311 – 319; d) J. J. Cox, F. Reimann, A. K. Nicholas, G. Thornton, E. Roberts, K. Springell, G. Karbani, H. Jafri, J. Mannan, Y. Raashid, L. Al-Gazali, H. Hamamy, E. M. Valente, S. Gorman, R. Williams, D. P. McHale, J. N. Wood, F. M. Gribble, C. G. Woods, *Nature* **2006**, *444*, 894 – 898.

[47] a) M. A. Nassar, L. C. Stirling, G. Forlani, M. D. Baker, E. A. Matthews, A. H. Dickenson, J. N. Wood, *Proc. Natl. Acad. Sci. USA* **2004**, *101*, 12706 – 12711; b) J. P. H. Drenth, S. G. Waxman, *J. Clin. Invest.* **2007**, *117*, 3603 – 3609.

[48] a) S. D. Dib-Hajj, Y. Yang, J. A. Black, S. G. Waxman, *Nat. Rev. Neurosci.* **2013**, *14*, 49 – 62; b) S. D. Dib-Hajj, J. A. Black, S. G. Waxman, *Pain Med.* **2009**, *10*, 1260 – 1269.

[49] A. Nardi, N. Damann, T. Hertrampf, A. Kless, *ChemMedChem* **2012**, *7*, 1712 – 1740.

[50] a) J. Payandeh, T. M. Gamal El-Din, T. Scheuer, N. Zheng, W. A. Catterall, *Nature* **2012**, *468*, 135 – 139; b) J. Payandeh, T. Scheuer, N. Zheng, W. A. Catterall, *Nature* **2011**, *475*, 353 – 358.

[51] X. Zhang, W. Ren, P. DeCaen, C. Yan, X. Tao, L. Tang, J. Wang, K. Hasegawa, T. Kumasaka, J. He, J. Wang, D. E. Clapham, N. Yan, *Nature* **2012**, *486*, 130 – 134.

[52] E. C. McCusker, C. Bagnéris, C. E. Naylor, A. R. Cole, N. D'Avanzo, C. G. Nichols, B. A. Wallace, *Nat. Commun.* **2012**, *3*, 1102.

[53] D. Shaya, F. Findeisen, F. Abderemane-Ali, C. Arrigoni, S. Wong, S. R. Nurva, G. Loussouarn, D. L. Minor, Jr., *J. Mol. Biol.* **2014**, *426*, 467 – 483.

[54] P. S. Rogers, H. Rapoport, *J. Am. Chem. Soc.* **1980**, *102*, 7335 – 7339.

[55] a) J. L. Wong, R. Oesterlin, H. Rapoport, *J. Am. Chem. Soc.* **1971**, *93*, 7344 – 7345; b) F. E. Russell, *Fed. Proc.* **1967**, *26*, 1206, attributed to H. Rapoport, M. S. Brown, R. Oesterlin, W. Schuett, Abstracts, the 147th National Meeting of the American Chemical Society, Philadelphia, April 1964, p. 3N.

[56] a) J. Bordner, W. E. Thiessen, H. A. Bates, H. Rapoport, *J. Am. Chem. Soc.* **1975**, *97*, 6008 – 6012; b) E. J. Schantz, V. E. Ghazarossian, H. K. Schnoes, F. M. Strong, J. P. Springer, J. O. Pezzanite, J. Clardy, *J. Am. Chem. Soc.* **1975**, *97*, 1238 – 1239.

[57] P. Vale, *Phytochem. Rev.* **2010**, *9*, 525 – 535.

[58] C. Y. Kao, S. E. Walker, *J. Physiol.* **1982**, *323*, 619 – 637.

[59] F. E. Koehn, V. E. Ghazarossian, E. J. Schantz, H. K. Schnoes, F. M. Strong, *Bioorg. Chem.* **1981**, *10*, 412 – 428.

[60] B. M. Andresen, Ph.D. Thesis, Stanford University (USA), **2009**.

[61] a) Y. Shimizu, *Annu. Rev. Microbiol.* **1996**, *50*, 431 – 465; b) Y. Shimizu, S. Gupta, K. Masuda, L. Maranda, C. K. Walker, R. H. Wang, *Pure Appl. Chem.* **1989**, *61*, 513 – 516; c) Y. Shimizu, M. Kobayashi, A. Genenah, N. Ichihara, *Seafood Toxins, Vol. 262*; *ACS Symposium Series* (Ed.: E. Ragelis), American Chemical Society, Washington, **1984**, pp. 151 – 160.

[62] a) R. Kellmann, T. K. Mihali, Y. J. Jeon, R. Pickford, F. Pomati, B. A. Neilan, *Appl. Environ. Microbiol.* **2008**, *74*, 4044 – 4053; b) T. K. Mihali, R. Kellmann, B. A. Neilan, *BMC Biochem.* **2009**, *10*, 8; c) A. Stüken, R. J. Orr, R. Kellmann, S. A. Murray, B. A. Neilan, K. S. Jakobsen, *PLoS One* **2011**, *6*, e20096; d) T. K. Mihali, W. W. Carmichael, B. A. Neilan, *PLoS One* **2011**, *6*, e14657.

[63] For a recent review on the evolution of STX synthesis in cyanobacteria and dinoflagellates, see: J. D. Hackett, J. H. Wisecaver, M. L. Brosnahan, D. M. Kulis, D. M. Anderson, D. Bhattacharya, F. G. Plumley, D. L. Erdner, *Mol. Biol. Evol.* **2013**, *30*, 70 – 78.

[64] For a recent review of adaptive evolutionary responses to STX and related toxins, see M. C. Jost, D. M. Hillis, Y. Lu, J. W. Kyle, H. A. Fozzard, H. H. Zakon, *Mol. Biol. Evol.* **2008**, *25*, 1016 – 1024.

[65] Recent research has investigated the potential of aquaculture for STX production; see: J. A. Galvão, M. Oetterer, M. C. Bittencourt-Oliveira, S. Gouvêa-Barros, S. Hiller, K. Erler, B. Luckas, E. Pinto, P. Kujbida, *Toxicon* **2009**, *54*, 891 – 894.

[66] a) M. Yotsu-Yamashita, B. Schimmele, T. Yasumoto, *Biosci. Biotechnol. Biochem.* **1999**, *63*, 961 – 963; b) T. Yasumoto, M. Yotsu, M. Murata, H. Naoki, *J. Am. Chem. Soc.* **1988**, *110*, 2344 – 2345; c) J. H. Jang, M. Yotsu-Yamashita, *Toxicon* **2007**, *50*, 947 – 951; d) M. Yotsu-Yamashita, Y. Yamagishi, T. Yasumoto, *Tetrahedron Lett.* **1995**, *36*, 9329 – 9332.

[67] a) H. Tanino, T. Nakata, T. Kaneko, Y. Kishi, *J. Am. Chem. Soc.* **1977**, *99*, 2818 – 2819; b) Y. Kishi, *Heterocycles* **1980**, *14*, 1477 – 1495.

[68] S. M. Hannick, Y. Kishi, *J. Org. Chem.* **1983**, *48*, 3833 – 3835.

[69] a) Y. Yamada, D. Milijkovic, P. Wehrli, B. Golding, P. Löliger, R. Keese, K. Müller, A. Eschenmoser, *Angew. Chem.* **1969**, *81*,

301–306; *Angew. Chem. Int. Ed. Engl.* **1969**, *8*, 343–348; b) M. Roth, P. Dubbs, E. Götschi, A. Eschenmoser, *Helv. Chim. Acta* **1971**, *54*, 710–734.

[70] R. G. Neville, J. J. McGee, *Can. J. Chem.* **1963**, *41*, 2123–2129.

[71] C. Y. Hong, Y. Kishi, *J. Am. Chem. Soc.* **1992**, *114*, 7001–7006.

[72] P. A. Jacobi, M. J. Martinelli, S. Polanc, *J. Am. Chem. Soc.* **1984**, *106*, 5594–5598.

[73] P. A. Jacobi, A. Brownstein, M. Martinelli, K. Grozinger, *J. Am. Chem. Soc.* **1981**, *103*, 239–241.

[74] O. Iwamoto, T. Shinohara, K. Nagasawa, *Chem. Asian J.* **2009**, *4*, 277–285.

[75] a) J. J. Fleming, J. Du Bois, *J. Am. Chem. Soc.* **2006**, *128*, 3926–3927; b) J. J. Fleming, M. D. McReynolds, J. Du Bois, *J. Am. Chem. Soc.* **2007**, *129*, 9964–9975.

[76] A. Goti, M. Cacciarni, F. Cardona, A. Brandi, *Tetrahedron Lett.* **1999**, *40*, 2853–2856.

[77] O. Iwamoto, M. Sekine, H. Koshino, K. Nagasawa, *Heterocycles* **2006**, *70*, 107–112; b) J. Shimokawa, K. Shirai, A. Tanatani, Y. Hashimoto, K. Nagasawa, *Angew. Chem.* **2004**, *116*, 1585–1588; *Angew. Chem. Int. Ed.* **2004**, *43*, 1559–1562; c) J. Shimokawa, T. Ishiwata, K. Shirai, H. Koshino, A. Tanatani, T. Nakata, Y. Hashimoto, K. Nagasawa, *Chem. Eur. J.* **2005**, *11*, 6878–6888.

[78] V. R. Bhonde, R. E. Looper, *J. Am. Chem. Soc.* **2011**, *133*, 20172–20174.

[79] Y. Sawayama, T. Nishikawa, *Angew. Chem.* **2011**, *123*, 7314–7316; *Angew. Chem. Int. Ed.* **2011**, *50*, 7176–7178.

[80] a) R. L. Giles, J. D. Sullivan, A. M. Steiner, R. E. Looper, *Angew. Chem.* **2009**, *121*, 3162–3166; *Angew. Chem. Int. Ed.* **2009**, *48*, 3116–3126; b) M. J. Gainer, N. R. Bennett, Y. Takahashi, R. E. Looper, *Angew. Chem.* **2011**, *123*, 710–713; *Angew. Chem. Int. Ed.* **2011**, *50*, 684–687.

[81] a) P. Merino, A. Lanaspa, F. L. Merchan, T. Tejero, *Tetrahedron: Asymmetry* **1998**, *9*, 629–646; b) P. Merino, S. Franco, F. L. Merchan, T. Tejero, *J. Org. Chem.* **1998**, *63*, 5627–5630.

[82] Cyclic *N*-Boc carbamates have previously been reported to undergo ring-opening under similar conditions: T. Kunieda, T. Ishizuka, *Tetrahedron Lett.* **1987**, *28*, 4185–4188.

[83] Y. Sawayama, T. Nishikawa, *Synlett* **2011**, 651–654.

[84] A. P. Thottumkara, J. R. Walker, J. E. Merit, R. Thomas-Tran, D. S. Finkelstein, J. Du Bois, Manuscript in preparation.

[85] B. M. Andresen, J. Du Bois, *J. Am. Chem. Soc.* **2009**, *131*, 12524–12525.

[86] W. H. Parsons, Ph.D. Thesis, Stanford University (USA), **2013**.

[87] A. E. Ondrus, H.-l. D. Lee, S. Iwanaga, W. H. Parsons, B. M. Andresen, W. E. Moerner, J. Du Bois, *Chem. Biol.* **2012**, *19*, 902–912.

[88] W. H. Parsons, J. Du Bois, *J. Am. Chem. Soc.* **2013**, *135*, 10582–10585.

[89] For a recent review on C-H amination, see J. L. Roizen, M. E. Harvey, J. Du Bois, *Acc. Chem. Res.* **2012**, *45*, 911–922.

[90] C. G. Espino, P. M. Wehn, J. Chow, J. Du Bois, *J. Am. Chem. Soc.* **2001**, *123*, 6935–6936.

[91] a) Y. Shimizu, L. J. Buckley, M. Alam, Y. Oshima, W. E. Fallon, H. Kasai, I. Miura, V. P. Fullo, J. Nakanishi, *J. Am. Chem. Soc.* **1976**, *98*, 5414–5416; b) G. L. Boyer, E. J. Schantz, H. K. Schnoes, *J. Chem. Soc. Chem. Commun.* **1978**, 889–890.

[92] a) D. A. Doyle, J. M. Cabral, R. A. Pfuetzner, A. Kuo, J. M. Gulbis, S. L. Cohen, B. T. Chait, R. MacKinnon, *Science* **1998**, *280*, 69–77; b) R. MacKinnon, *Potassium Channels and the Atomic Basis of Selective Ion Conduction*, in *Les Prix Nobel. The Nobel Prizes 2003* (Ed.: T. Frängsmyr), Stockholm, **2004**; c) R. MacKinnon, *Angew. Chem.* **2004**, *116*, 4363–4376; *Angew. Chem. Int. Ed.* **2004**, *43*, 4265–4277.

[93] a) C. Sato, Y. Ueno, K. Asai, K. Takahashi, M. Sato, A. Engel, Y. Fujiyoshi, *Nature* **2001**, *409*, 1047–1051; b) C. Sato, M. Sato, A. Iwasaki, T. Doi, A. Engel, *J. Struct. Biol.* **1998**, *121*, 314–325.

[94] M. Noda, S. Shimizu, T. Tanabe, T. Takai, T. Kayano, T. Ikeda, H. Takahashi, H. Nakayama, Y. Kanaoka, N. Minamino, K. Kangawa, H. Matsuo, M. A. Raftery, T. Hirose, S. Inayama, H. Hayashida, T. Miyata, S. Numa, *Nature* **1984**, *312*, 121–127.

[95] H. R. Guy, P. Seetharamulu, *Proc. Natl. Acad. Sci. USA* **1986**, *83*, 508–512.

[96] a) B. Hirschberg, A. Rovner, M. Lieberman, J. Patlak, *J. Gen. Physiol.* **1995**, *106*, 1053–1068; b) N. Yang, A. L. George, Jr., R. Horn, *Neuron* **1996**, *16*, 113–122.

[97] J. W. West, D. E. Patton, T. Scheuer, Y. Wang, A. L. Goldin, W. A. Catterall, *Proc. Natl. Acad. Sci. USA* **1992**, *89*, 10910–10914.

[98] a) I. Favre, E. Moczydlowski, L. Schild, *Biophys. J.* **1996**, *71*, 3110–3125; b) T. Schlief, R. Schönherr, K. Imoto, S. H. Heinemann, *Eur. Biophys. J.* **1996**, *25*, 75–91; c) Y.-M. Sun, I. Favre, L. Schild, E. Moczydlowski, *J. Gen. Physiol.* **1997**, *110*, 693–715.

[99] Figure taken from G. F. King, P. Escoubas, G. M. Nicholson, *Channels* **2008**, *2*, 100–116.

[100] B. Hille, *J. Gen. Physiol.* **1971**, *58*, 599–619.

[101] B. Hille, *Biophys. J.* **1975**, *15*, 615–619.

[102] R. Henderson, J. M. Ritchie, G. R. Strichartz, *Proc. Natl. Acad. Sci. USA* **1974**, *71*, 3936–3940.

[103] For additional competition experiments that enabled elucidation of the channel pore, see: a) R. L. Barchi, J. B. Wiegele, *J. Physiol.* **1979**, *295*, 383–396; b) W. A. Catterall, C. S. Morrow, R. P. Hartshorne, *J. Biol. Chem.* **1979**, *254*, 11379–11387.

[104] M. Noda, T. Ikeda, T. Kayano, H. Suzuki, H. Takeshima, M. Kurasaki, H. Takahashi, S. Numa, *Nature* **1986**, *320*, 188–192.

[105] J. S. Trimmer, S. S. Cooperman, S. A. Tomiko, J. Zhou, S. M. Crean, M. B. Boyle, R. G. Kallen, Z. Sheng, R. Barchi, F. J. Sigworth, R. H. Goodman, W. S. Agnew, G. Mandel, *Neuron* **1989**, *3*, 33–49.

[106] M. Noda, H. Suzuki, S. Numa, W. Stühmer, *FEBS Lett.* **1989**, *259*, 213–216.

[107] a) H. Terlau, S. H. Heinemann, W. Stühmer, M. Pusch, F. Conti, K. Imoto, S. Numa, *FEBS Lett.* **1991**, *293*, 93–96; b) M. Pusch, M. Noda, W. Stühmer, S. Numa, F. Conti, *Eur. Biophys. J.* **1991**, *20*, 127–133; c) K. J. Kontis, A. L. Goldin, *Mol. Pharmacol.* **1993**, *43*, 635–644; d) M. M. Stephan, J. F. Potts, W. S. Agnew, *J. Membr. Biol.* **1994**, *137*, 1–8.

[108] S. H. Heinemann, H. Terlau, W. Stühmer, K. Imoto, S. Numa, *Nature* **1992**, *356*, 441–443.

[109] J. Yang, P. T. Ellinor, W. A. Sather, J.-F. Zhang, R. W. Tsien, *Nature* **1993**, *366*, 158–161.

[110] C. M. Bay, G. R. Strichartz, *J. Physiol.* **1980**, *300*, 89–103.

[111] L. L. Cribbs, J. Satin, H. A. Fozzard, R. B. Rogart, *FEBS Lett.* **1990**, *275*, 195–200.

[112] P. H. Backx, D. T. Yue, J. H. Lawrence, E. Marban, G. F. Tomaselli, *Science* **1992**, *257*, 248–251.

[113] S. H. Heinemann, H. Terlau, K. Imoto, *Pfluegers Arch. Eur. J. Physiol.* **1992**, *422*, 90–92.

[114] I. Favre, E. Moczydlowski, L. Schild, *J. Gen. Physiol.* **1995**, *106*, 203–229.

[115] L. Sivilotti, K. Okuse, A. N. Akopian, S. Moss, J. N. Wood, *FEBS Lett.* **1997**, *409*, 49–52.

[116] V. P. Santarelli, A. L. Eastwood, D. A. Dougherty, R. Horn, C. A. Ahern, *J. Biol. Chem.* **2007**, *282*, 8044–8051.

[117] For a recent review of the TTX binding site, see: H. A. Fozzard, G. M. Lipkind, *Mar. Drugs* **2010**, *8*, 219–234.

[118] M. Yotsu-Yamashita, K. Nishimori, Y. Nitanai, M. Isemura, A. Sugimoto, T. Yasumoto, *Biochem. Biophys. Res. Commun.* **2000**, *267*, 403–412.

[119] V. M. Bricelj, L. Connell, K. Konoki, S. P. MacQuarrie, T. Scheuer, W. A. Catterall, V. L. Trainer, *Nature* **2005**, *434*, 763–767.

[120] C. R. Feldman, E. D. Brodie, Jr., E. D. Brodie III, M. E. Pfrender, *Proc. Natl. Acad. Sci. USA* **2012**, *109*, 4556–4561.

[121] J. L. Penzotti, H. A. Fozzard, G. M. Lipkind, S. C. Dudley, Jr., *Biophys. J.* **1998**, *75*, 2647–2657.

[122] J. R. Walker, P. Novick, W. H. Parsons, M. MacGregor, J. Zablocki, V. S. Pande, J. Du Bois, *Proc. Natl. Acad. Sci. USA* **2012**, *109*, 18102–18107.

[123] C. T. Hanifin, *Mar. Drugs* **2010**, *8*, 577–593.

[124] C. Y. Kao, S. E. Walker, *J. Physiol.* **1982**, *323*, 619–637.

[125] Y. Shimizu, C.-p. Hsu, W. E. Fallon, Y. Oshima, I. Miura, K. Nakanishi, *J. Am. Chem. Soc.* **1978**, *100*, 6791–6793.

[126] G. Strichartz, *J. Gen. Physiol.* **1984**, *84*, 281–305.

[127] E. Moczydlowski, S. Hall, S. S. Garber, G. S. Strichartz, C. Miller, *J. Gen. Physiol.* **1984**, *84*, 687–704.

[128] C. Y. Kao, P. N. Kao, M. R. James-Kracke, F. E. Koehn, C. F. Wichmann, H. K. Schnoes, *Toxicon* **1985**, *23*, 647–655.

[129] S. L. Hu, C. Y. Kao, F. E. Koehn, H. K. Schnoes, *Toxicon* **1987**, *25*, 159–165.

[130] C. Y. Kao, *Ann. N. Y. Acad. Sci.* **1986**, *479*, 52–67.

[131] G. Choudhary, M. Yotsu-Yamashita, L. Shang, T. Yasumoto, S. C. Dudley, Jr., *Biophys. J.* **2003**, *84*, 287–294.

[132] D. B. Tikhonov, B. S. Zhorov, *Mol. Pharmacol.* **2012**, *82*, 97–104.

[133] a) G. M. Lipkind, J. A. Fozzard, *Biochemistry* **2000**, *39*, 8161–8170; b) G. M. Lipkind, J. A. Fozzard, *J. Gen. Physiol.* **2008**, *131*, 523–529.

[134] V. E. Ghazarossian, E. J. Schantz, H. K. Schnoes, F. M. Strong, *Biochem. Biophys. Res. Commun.* **1976**, *68*, 776–780.

[135] R. Thomas-Tran, J. Du Bois, Unpublished data.

[136] a) L. E. Llewellyn, P. M. Bell, E. G. Moczydlowski, *Proc. R. Soc. London Ser. B* **1997**, *264*, 891–902; b) C. Robillot, D. Kineavy, J. Burnell, L. E. Llewellyn, *Toxicon* **2009**, *53*, 460–465.

[137] R. Watanabe, R. Samusawa-Saito, Y. Oshima, *Bioconjugate Chem.* **2006**, *17*, 459–465.

[138] R. Shinohara, T. Akimoto, O. Iwamoto, T. Hirokawa, M. Yotsu-Yamashita, K. Yamaoka, K. Nagasawa, *Chem. Eur. J.* **2011**, *17*, 12144–12152.

[139] T. Akimoto, A. Masuda, M. Yamashita, T. Hirokawa, K. Nagasawa, *Org. Biomol. Chem.* **2013**, *11*, 6642–6649.

[140] Y. Kudo, T. Yasumoto, K. Konoki, Y. Cho, M. Yotsu-Yamashita, *Mar. Drugs* **2012**, *10*, 655–667.

[141] "The Chemistry of Tetrodotoxin": H. S. Mosher in *Tetrodotoxin, Saxitoxin, and the Molecular Biology of the Sodium Channel, Vol. 479* (Eds.: C. Y. Kao, S. R. Levinson), Annals of the New York Academy of Science, New York, **1986**.

[142] a) H. Nakayama, E. Yoshida, Y. Kanaoka, *Chem. Pharm. Bull.* **1986**, *34*, 2684–2686; b) E. Yoshida, H. Nakayama, Y. Hatanaka, Y. Kanaoka, *Chem. Pharm. Bull.* **1990**, *38*, 982–987; c) H. Nakayama, Y. Hatanaka, E. Yoshida, K. Oka, M. Takanohashi, Y. Amano, Y. Kanaoka, *Biochem. Biophys. Res. Commun.* **1992**, *184*, 900–907.

[143] K. Tsuda, S. Ikuma, M. Kawamura, R. Tachikawa, K. Sakai, C. Tamura, O. Amakasu, *Chem. Pharm. Bull. Jpn.* **1964**, *12*, 1357–1374.

[144] T. Goto, Y. Kishi, S. Takahashi, Y. Hirata, *Tetrahedron* **1965**, *21*, 2059–2088.

[145] C. Rosker, B. Lohberger, D. Hofer, B. Steinecker, S. Quasthoff, W. Schreibmayer, *Am. J. Physiol. Cell Physiol.* **2007**, *293*, C783–C789.

[146] G. Choudhary, L. Shang, X. Li, S. C. Dudley, Jr., *Biophys. J.* **2002**, *83*, 912–919.

[147] G. Choudhary, M. P. Aliste, D. P. Tieleman, R. J. French, S. C. Dudley, *Channels* **2007**, *1*, 344–352.

[148] G. M. Lipkind, J. A. Fozzard, *Biophys. J.* **1994**, *66*, 1–13.

[149] a) D. B. Tikhonov, B. S. Zhorov, *Biophys. J.* **2005**, *88*, 184–197; b) D. B. Tikhonov, B. S. Zhorov, *J. Biol. Chem.* **2011**, *286*, 2998–3006.

[150] S. A. Shankarappa, J. H. Tsui, K. N. Kim, G. Reznor, J. C. Dohlman, R. Langer, D. S. Kohane, *Proc. Natl. Acad. Sci. USA* **2012**, *109*, 17555–17560.

[151] For representative reports of the application of GTX in the treatment of pain, see: a) R. Garrido, N. Lagos, M. Lagos, A. J. Rodriguez-Navarro, C. Garcia, D. Truan, A. Henriquez, *Colorectal Dis.* **2007**, *9*, 619–624; b) R. Garrido, N. Lagos, K. Lattes, M. Abedrapo, G. Bocic, A. Cuneo, H. Chiong, C. Jensen, R. Azolas, A. Henriquez, C. Garcia, *Dis. Colon Rectum* **2005**, *48*, 335–343; c) K. Lattes, P. Venegas, N. Lagos, M. Lagos, L. Pedraza, A. J. Rodriguez-Navarro, C. Garcia, *Neurol. Res.* **2009**, *31*, 228–233.

[152] For representative reports of the application of neo-STX in humans for pain treatment, see: a) A. J. Rodriguez-Navarro, M. Lagos, C. Figueroa, C. Garcia, P. Recebal, P. Silva, V. Iglesias, N. Lagos, *Neurotoxic. Res.* **2009**, *16*, 408–415; b) A. J. Rodriguez-Navarro, N. Lagos, M. Lagos, I. Braghetto, A. Csendes, J. Hamilton, C. Figueroa, D. Truan, C. Garcia, A. Rojas, V. Iglesias, L. Brunet, F. Alvarez, *Anesthesiology* **2007**, *106*, 339–345; c) A. J. Rodriguez-Navarro, C. B. Berde, G. Wiedmaier, A. Mercado, C. Garcia, V. Iglesias, D. Zurakowski, *Reg. Anesth. Pain Med.* **2011**, *36*, 103–109.

[153] G. R. Strichartz, S. Hall, B. Magnani, C. Y. Hong, Y. Kishi, J. A. Debin, *Toxicon* **1995**, *33*, 723–737.

[154] R. Stämpfli, *Experientia* **1954**, *10*, 508–509.

[155] For descriptions of this cell line, see: a) K. Kogure, M. L. Tamplin, U. Simidu, R. R. Colwell, *Toxicon* **1988**, *26*, 191–197; M. Yotsu-Yamashita, D. Urabe, M. Asai, T. Nishikawa, M. Isobe, *Toxicon* **2003**, *42*, 557–560.

[156] H. Mao, L. A. Fieber, R. E. Gawley, *ACS Med. Chem. Lett.* **2010**, *1*, 135–138.

[157] J. W. Schmidt, W. A. Catterall, *J. Biol. Chem.* **1987**, *262*, 13713–13723.

[158] A. Hoehne, D. Behera, W. H. Parsons, M. L. James, B. Shen, P. Borgohain, D. Bodapati, A. Prabhakar, S. S. Gambhir, D. C. Yeomans, S. Biswal, F. T. Chin, J. Du Bois, *J. Am. Chem. Soc.* **2013**, *135*, 18012–18015.

[159] For representative discussions on the use of anesthetics to target Na$_V$, see: a) A. Scholz, *Br. J. Anaesth.* **2002**, *89*, 52–61; b) K. F. Herold, H. C. Hemmings, Jr., *Front. Pharmacol.* **2012**, *3*, 50.

[160] GFP labeling of individual Na$_V$ isoforms has been accomplished; see: a) T. Zimmer, C. Biskup, C. Bollensdorff, K. Benndorf, *J. Membr. Biol.* **2002**, *186*, 13–21; b) T. Zimmer, C. Biskup, S. Dugarmaa, F. Vogel, M. Steinbis, T. Böhle, Y. S. Wu, R. Dumaine, K. Benndorf, *J. Membr. Biol.* **2002**, *186*, 1–12; c) H. Hallaq, Z. Yang, P. C. Viswanathan, K. Fukuda, W. Shen, D. W. Wang, K. S. Wells, J. Zhou, J. Yi, K. T. Murray, *Cardiovasc. Res.* **2006**, *72*, 250–261; d) A. Gasser, T. S.-Y. Ho, X. Cheng, K.-J. Chang, S. G. Waxman, M. N. Rasband, S. D. Dibb-Hajj, *J. Neurosci.* **2012**, *32*, 7232–7243.

[161] For representative reports on challenges associated with GFP-Na$_V$ fusion proteins, see: a) R. Maue, *J. Cell. Physiol.* **2007**, *213*, 618–623; b) B. J. Baker, H. Lee, V. A. Pieribone, L. B. Cohen, E. Y. Isacoff, T. Knopfel, E. K. Kosmidis, *J. Neurosci. Methods* **2007**, *161*, 32–38; c) G. G. Schofield, H. L. Puhl III, S. R. Ikeda, *J. Neurophysiol.* **2008**, *99*, 1917–1927; d) K. Ataka, V. A. Pieribone, *Biophys. J.* **2002**, *82*, 509–516.

[162] For recent reports on the use of TTX in human trials for pain management, see: a) N. A. Hagen, K. M. Fisher, B. Lapointe, P. du Souich, S. Chary, D. Moulin, E. Sellers, A. H. Ngoc, *J. Pain Symptom Manage.* **2007**, *34*, 171–182; b) N. A. Hagen, P. du Souich, B. Lapointe, M. Ong-Lam, B. Dubuc, D. Walde, *J. Pain Symptom Manage.* **2008**, *35*, 420–429.